Exceptional service in the national interest

SAND2018-1958PE

Sandia National Laboratories

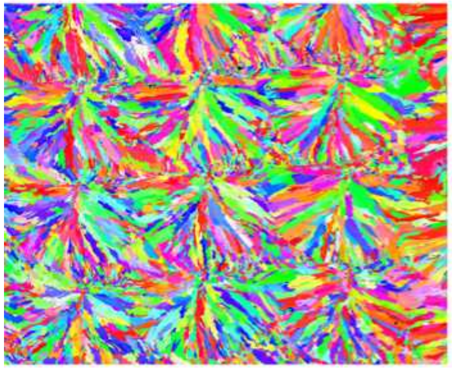

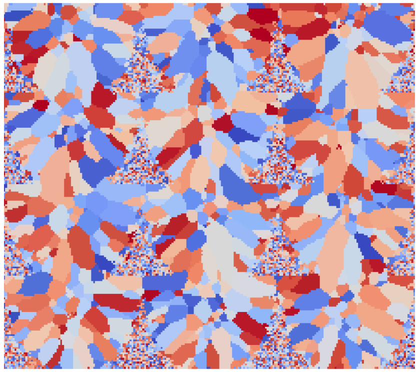

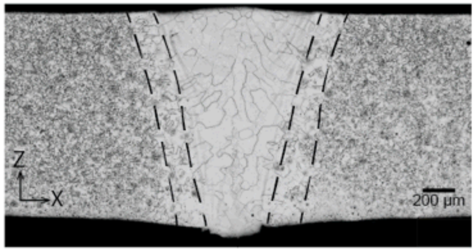

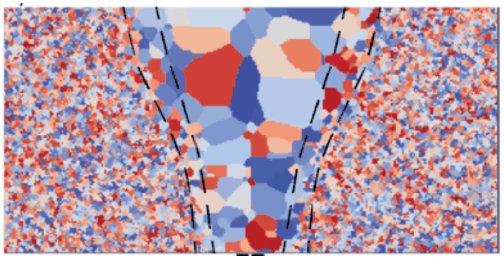

Simulating Microstructural Evolution during Metal Additive Manufacturing

Theron Rodgers

Sandia National Laboratories is a multimission laboratory managed and operated by National Technology & Engineering Solutions of Sandia, LLC, a wholly owned subsidiary of Honeywell International, Inc., for the U.S. Department of Energy's National Nuclear Security Administration under contract DE-NA0003525.

Collaborators

- Sandia National Laboratories, New Mexico
  - Jonathan Madison
  - Kyle Johnson
  - John Mitchell
  - Veena Tikare
  - Svetoslov Nikolov
  - Hojun Lim
  - Joseph Bishop
  - Olivia Underwood
  - Bradley Jared
  - Joseph Michael
- Georgia Tech
  - Evdokia Popova
  - Xinyi Gong
  - Ahmet Cecen
  - Surya Kalidindi

Outline

- Motivation
- Introduction to Monte Carlo-based microstructure modeling
- Application to solidification problems
- Using synthetic microstructures in further analysis
- Recent & on-going work

Metal Additive Manufacturing Background

IR movies of LENS build (D. Dagel, SNL)

Different Powder Bed Scan Paths for Cylinder (B. Jared, SNL)

- A 3D CAD model is sliced into 2D layers, which are segmented into individual heat source (laser, electron beam, etc) paths.
- The path file is programmed into a build machine that constructs the component layer-by-layer.
- There are 2 general categories of AM machines: powder bed and powder/wire fed.

AM builds have many sources of variation.

Variation through build domain

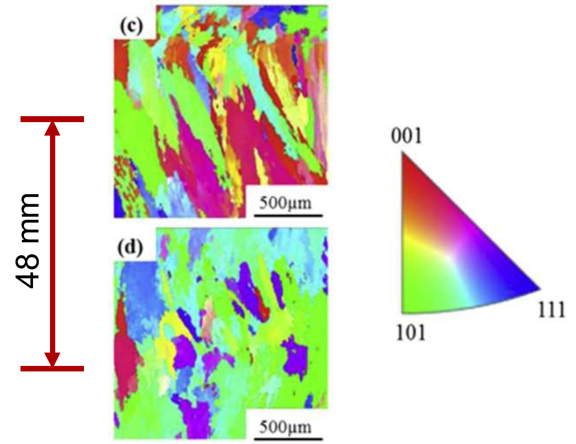

Z. Wang et al., ***Acta Mater. 2016***

Variation with differing geometries

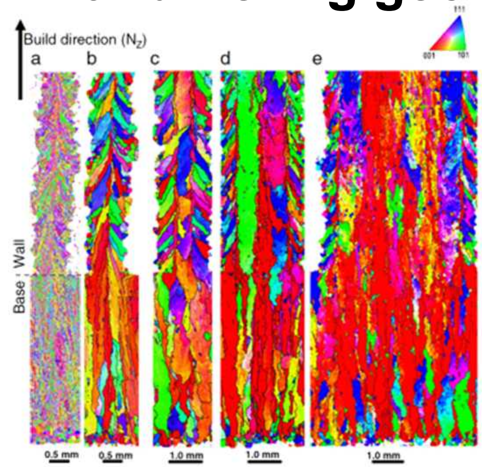

A. Antonysamy et al., ***Mater. Charact. 2013***

Variation due to scan pattern

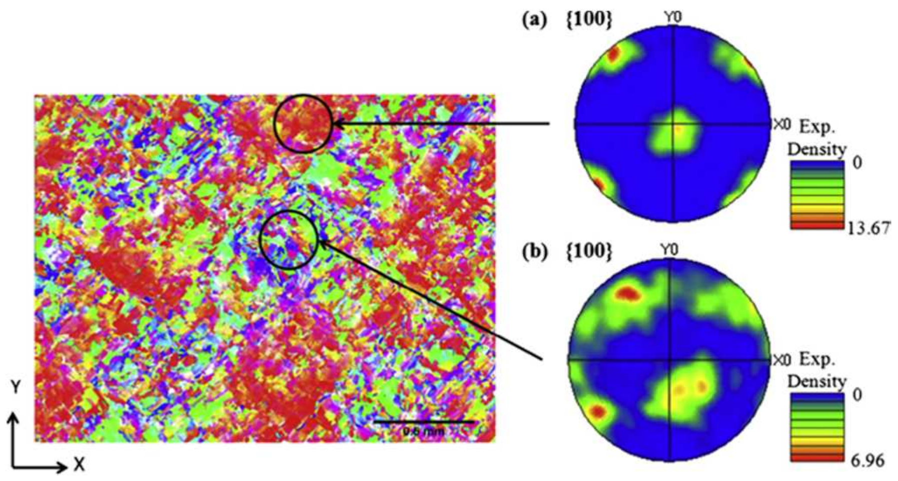

L. Carter et al., ***J. Alloys Compd. 2014***

Variation with processing conditions

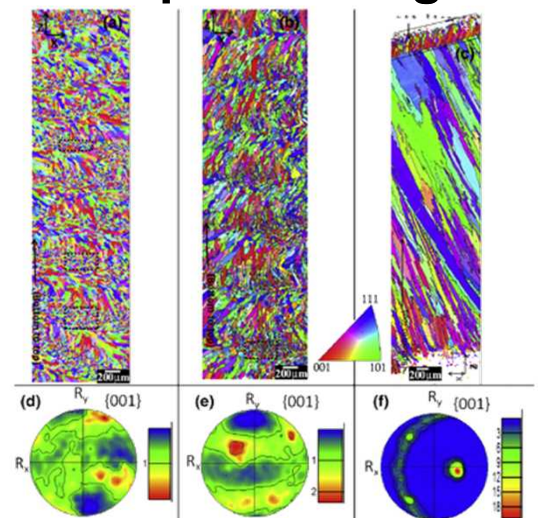

Parimi et al., ***Mater. Charact. 2014***

AM material simulation methods exist at many length and time scales

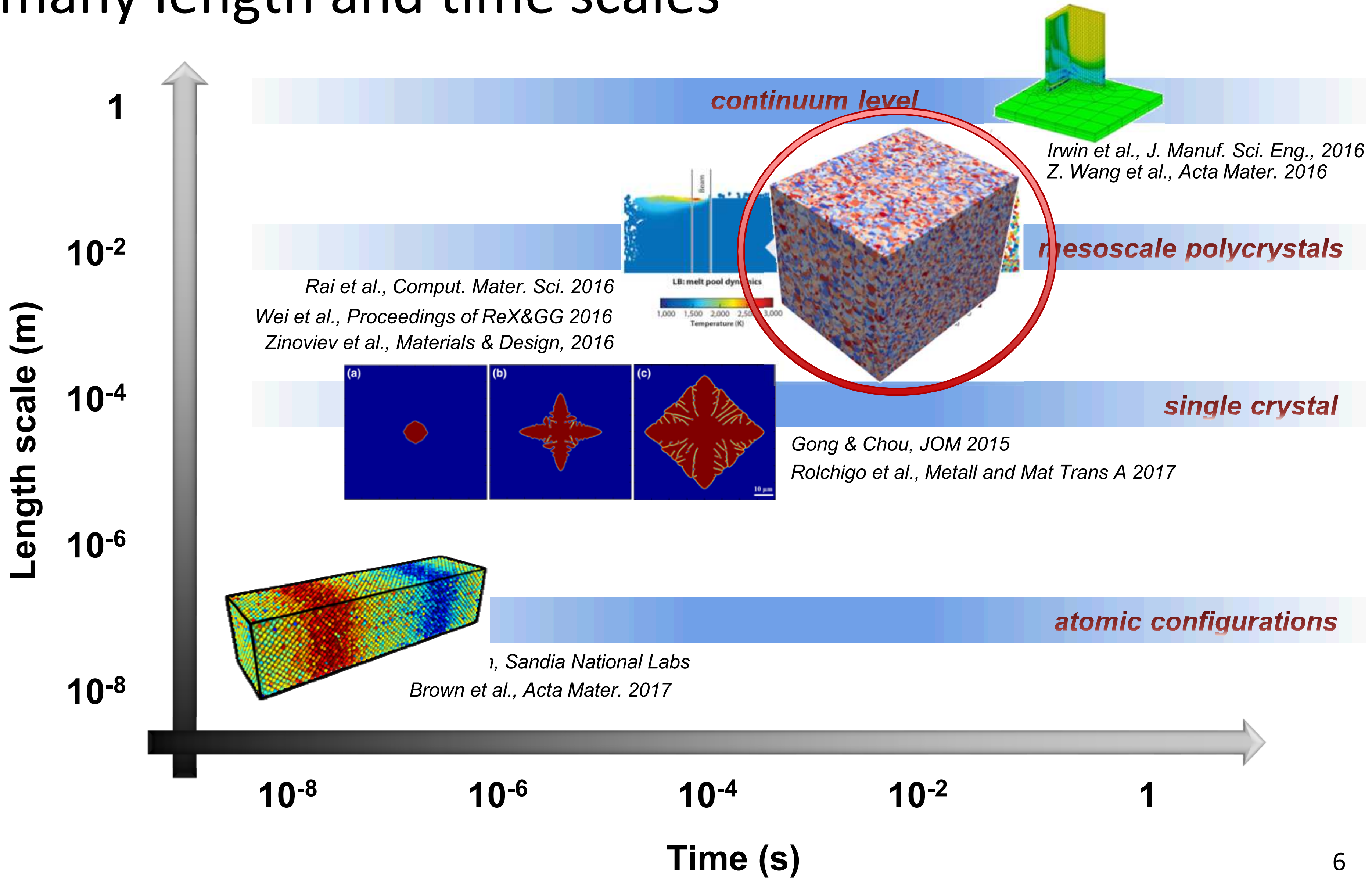

Simulation Framework

SPPARKS

Kinetic Monte Carlo via Stochastic Parallel PARticle Kinetic Simulator

- Open source kinetic Monte Carlo platform with user-editable “apps” for specific applications
- Used to study several mesoscale phenomena including sintering, recrystallization, vacancy diffusion, grain growth and welding
- Problems are easily parallelized and a range of Monte Carlo solvers are available

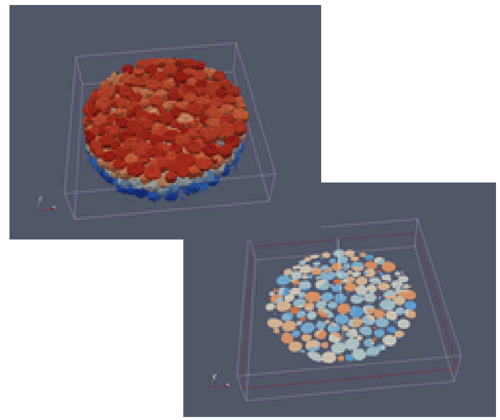

Tikare & Garcia-Cardona

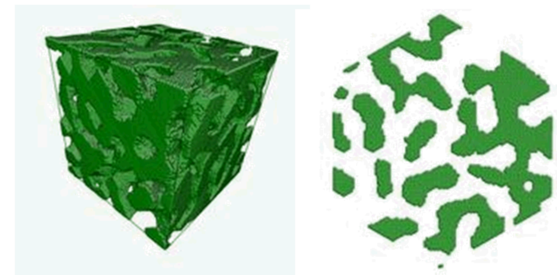

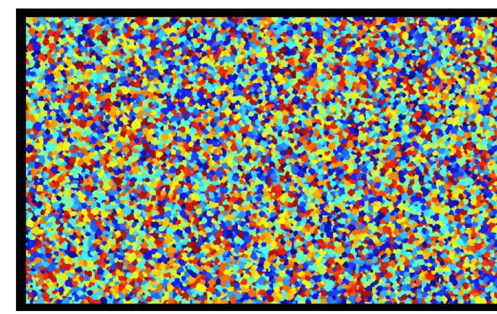

Rodgers, Madison, & Tikare

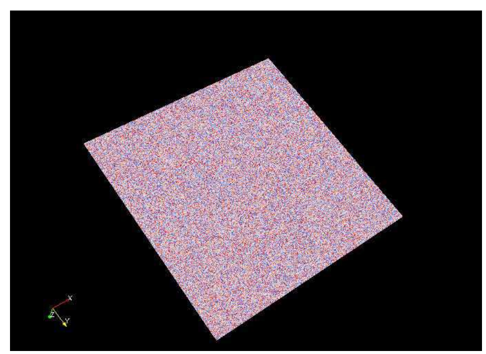

spparks.sandia.gov

SNL Modeling Work

Codes
LAMMPS, SPPARKS,
Sierra/Aria, Sierra/Adagio

Powder Behavior
Mark Wilson

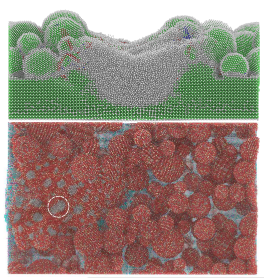

Powder Spreading
Dan Bolintineanu

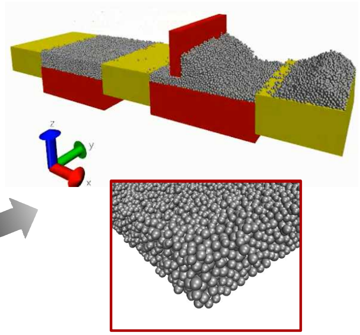

Mesoscale Thermal Behavior
Mario Martinez , Dan Moser & Brad Trembacki

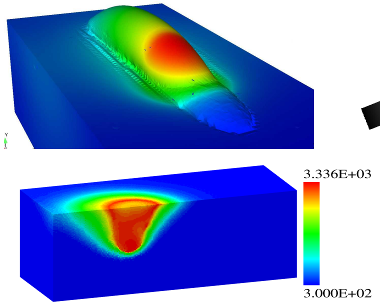

Mesoscale Texture/Solid Mechanics/CX
Judy Brown, Theron Rodgers and Kurtis Ford

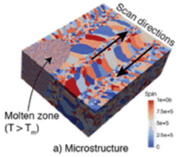

Part Scale Thermal & Solid Mechanics
Kyle Johnson, Kurtis Ford & Joe Bishop

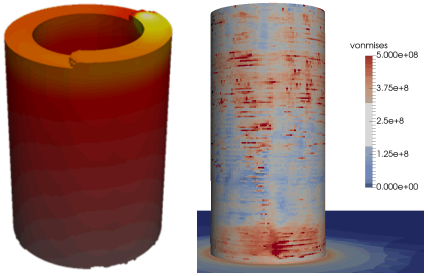

Part Scale Microstructure
Theron Rodgers

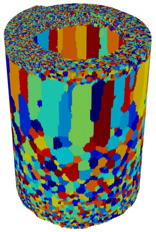

10^{-6} 10^{-3} 1

Length Scale (m)

The KMC method & AM

$$M(T) = M_o \exp\left(\frac{-Q}{RT}\right)$$

$$P = \begin{cases} M(T)\exp\left(\frac{-\Delta E}{k_B T_s}\right), & if\ \Delta E > 0 \\ M(T), & if\ \Delta E \leq 0 \end{cases}$$

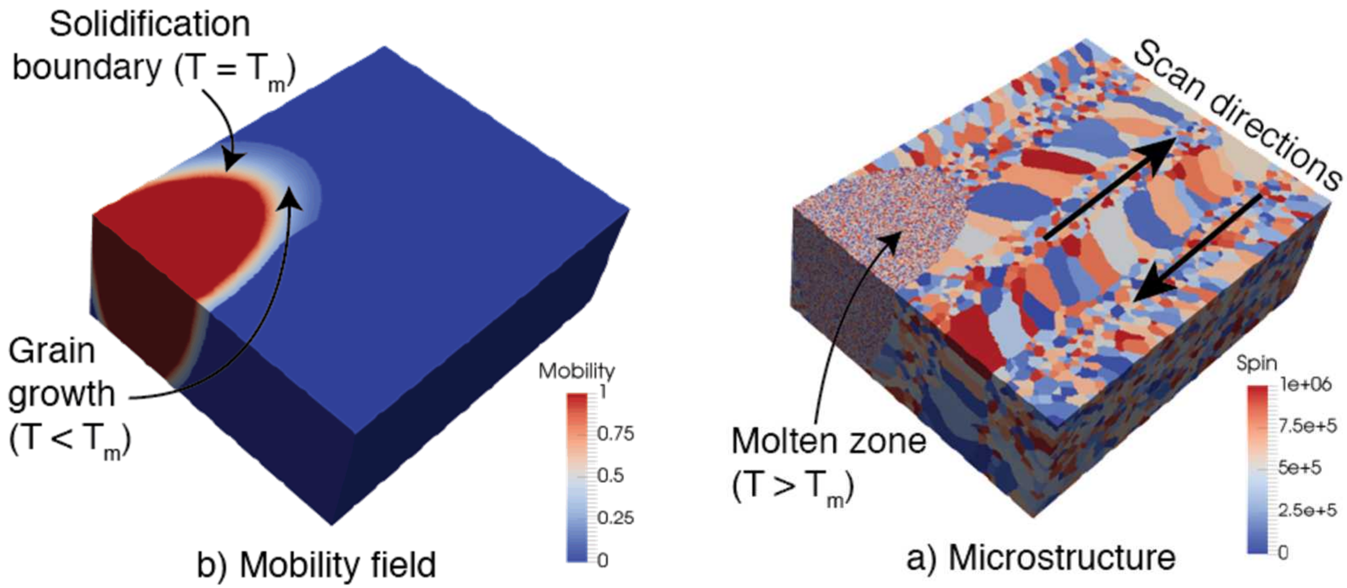

- The molten zone randomizes grain identities when it enters a region.
- Along the trailing surface, voxels either join existing columnar grains or form new grains.
- The temperature gradient creates a corresponding gradient of grain boundary mobilities via an Arrhenius relationship.

Heat source interactions

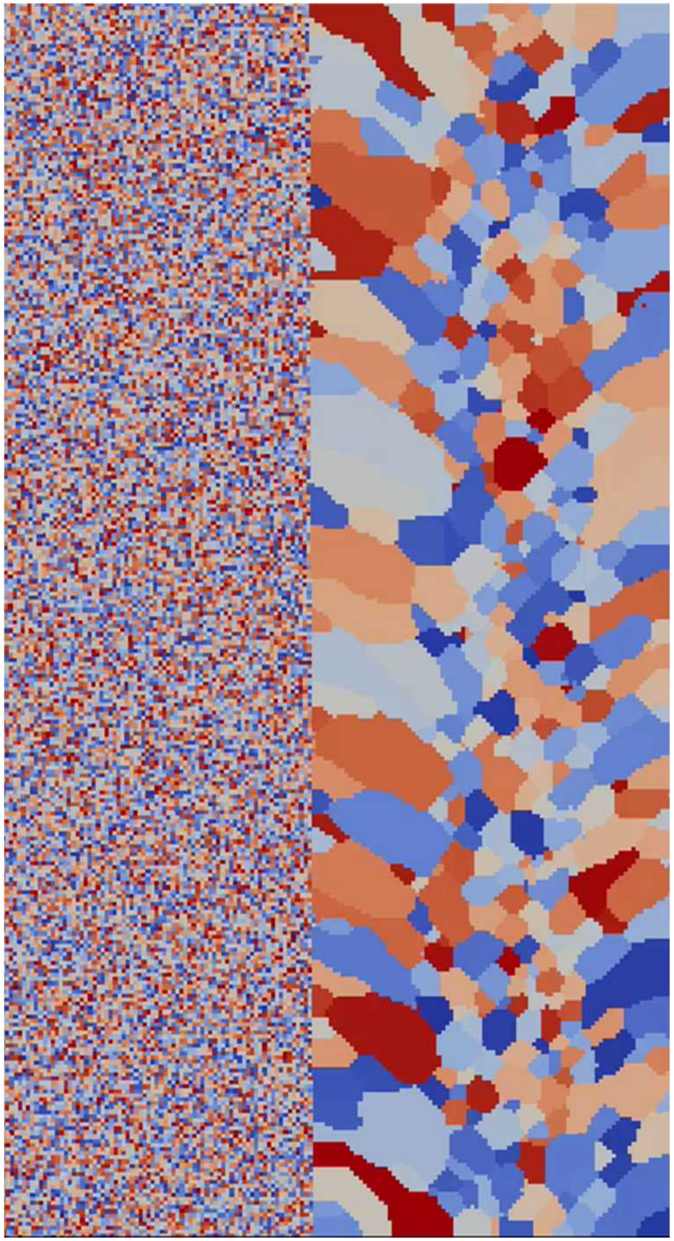

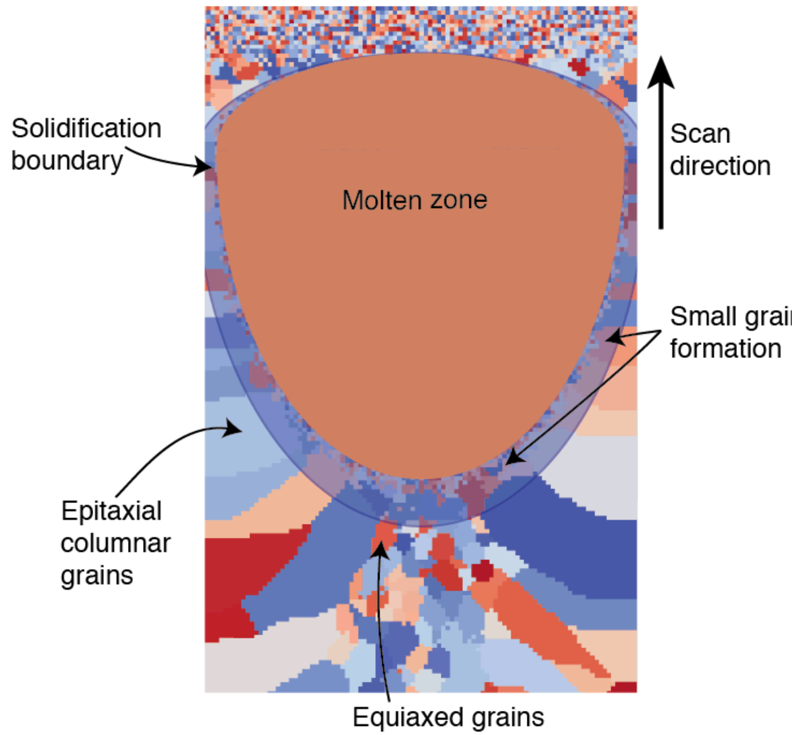

AM & Weld models avail at spparks.sandia.gov

app_style potts/weld command

Syntax:

app_style style nspins yp alpha beta velocity haz

- style = potts/weld
- nspins = number of possible Potts model spins
- yp = initial melt pool position along y-axis
- alpha = controls relative size of melt pool shape at bottom compared to top
- beta = Bezier control point parameter that defines curvature of melt pool shape through thickness
- velocity = velocity of melt pool motion (lattice sites per Monte Carlo step)
- haz = width of the heat affected zone (haz) surrounding the melt pool

Examples:

```
app_style potts/weld 10000 0 0.5 0.75 7.0 50.0
weld_shape_ellipse 100.0 150.0
```

This defines a potts/weld model with 10000 spins. An elliptical pool shape is specified with width and length of 100 and 150 sites respectively; note these are pool dimensions at the top surface of the weld. The value *alpha=0.5* scales the elliptical pool width and length at the top surface to 50 and 75 sites respectively at the bottom (root) surface of the weld. The Bezier control point parameter specifies an outwardly curved pool; the weld speed is 7 MCS and the heat effect zone is 50 sites wide.

This application also requires one of the following commands to specify pool geometry:

weld_shape_ellipse	specify elliptical pool shape parameters
weld_shape_teardrop	specify teardrop pool shape parameters

Description:

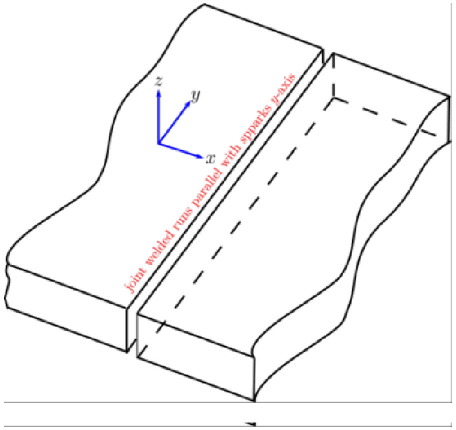

SPPARKS WWW Site - SPPARKS Documentation - SPPARKS Commands

app_style potts/additive command

Syntax:

```
app_style potts/additive nspins spot_width melt_tail_length melt_depth cap_height HAZ tail_HAZ depth_HAZ cap_HAZ exp_factor
```

- potts/additive = application style name
- nspins = number of possible spins
- spot_width = maximum width of the melt pool
- melt_tail_length = maximum length of the melt pool trailing the melt spot
- melt_depth = maximum depth of the melt pool
- cap_height = maximum length of the melt pool leading the melt spot
- HAZ = width of the heat affected zone (haz) surrounding the melt pool (must be larger than width)
- tail_HAZ = Length of the haz trailing the meltpool (must be larger than tail_length)
- depth_HAZ = depth of the heat affect zone (haz) below the melt pool (must be larger than depth)
- cap_HAZ = Length of haz leading the melt pool (must be larger than cap_length)
- exp_factor = Coefficient that controls the rate of exponential decay of the haz mobility gradient

Examples:

app_style potts/additive 1000 30 40 20 5 50 60 30 7 0.1

Description:

This is an on-lattice application derived from the app_style potts/neighonly application that simulates the rastering of a molten pool and its accompanying heat-affected zone (HAZ) through a domain. Rastering is achieved through the specification of layer-by-layer patterns, which can be combined into an overall pattern specifying the translation of the molten zone through the entire simulation domain. The application allows for arbitrary numbers of paths in each layer and an arbitrary number of layers in each pattern. Thus, the user can construct any scan strategy desired by specifying individual layer patterns and how these patterns should be repeated.

The molten pool is defined as a double ellipsoid. The ellipsoids share identical values for two of their axes (defined by the *melt_width* and *melt_depth* parameters). The third axis of each ellipsoid is defined by either the *melt_tail_length* or *cap_height* parameters. The haz is also defined by four equivalent parameters: *HAZ*, *tail_HAZ*, *depth_HAZ*, and *cap_HAZ*. A schematic of these eight parameters is shown below.

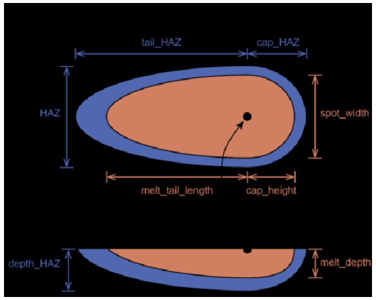

The model also requires specification of the *exp_factor* variable, which determines the value of the coefficient in the mobility equation, $M = exp(-exp\_factor * x)$, where x is the shortest distance from the lattice site to the molten pool boundary.

This application was used in the paper by Rodgers and collaborators.

The following additional commands are defined by this application, and in fact must be specified to setup a simulation.

am_pass	Define the parameters for each type of single-track pass.
am_transverse_pass	Define the parameters for the transverse increment (a.k.a. hatch spacing) between each pass.
am_cartesian_layer	Define the combination of passes and transverse_passes that comprise a layer. Limited to passes aligned along the +/-X or Y axes.
am_pattern	Define the combination of layers that comprise a pattern.

The examples/potts_additive directory has input files which illustrate how to use these additional commands.

Restrictions:

This application is only compatible with square and square cubic lattices.

This application can only be evolved by a rejection KMC (rKMC) algorithm. See the sweep command for more details.

The settings for melt pool width + haz must be <= xhi & yhi.

Related commands:

app_style potts/weld, app_style potts/weld/jom

Default: none

(Rodgers) T.M. Rodgers, J.D. Madison and V. Tikare, "Simulation of Metal Additive Manufacturing Microstructures Using Kinetic Monte Carlo", Computational Materials Science (2017).

Outline

- Motivation
- Introduction to Monte Carlo-based microstructure modeling
- Application to solidification problems
  - **Electron beam & laser welding**
  - Additive manufacturing
- Using synthetic microstructures in further analysis
- Recent & on-going work

Details of the model

- Grains are randomized upon entry to melt region
- New grains solidify along trailing edge of melt region
- Grain growth occurs in hot zone surrounding melt region

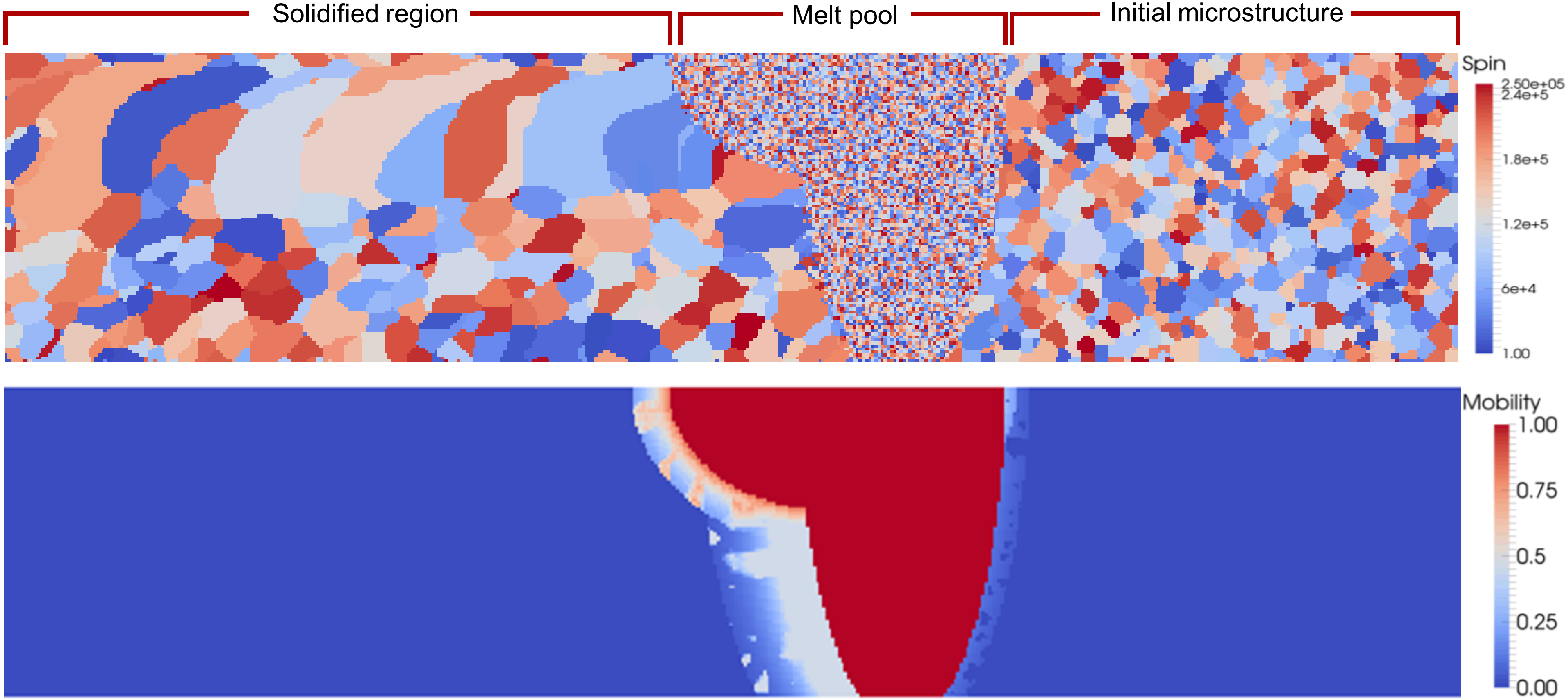

Rodgers, et al., ***JOM 2016***

Details of the model

- Grains are randomized upon entry to melt region
- New grains solidify along trailing edge of melt region
- Grain growth occurs in hot zone surrounding melt region

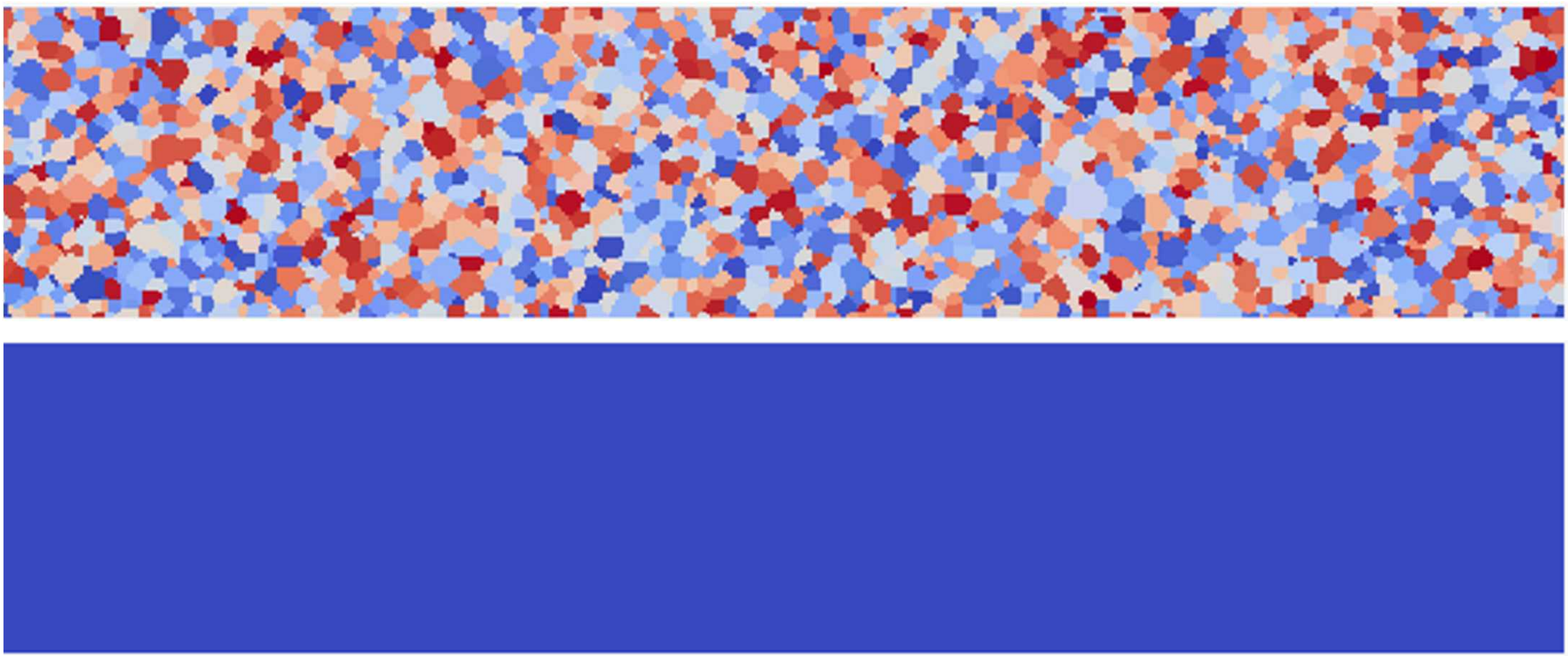

Rodgers, et al., ***JOM 2016***

Electron Beam weld cross-sections

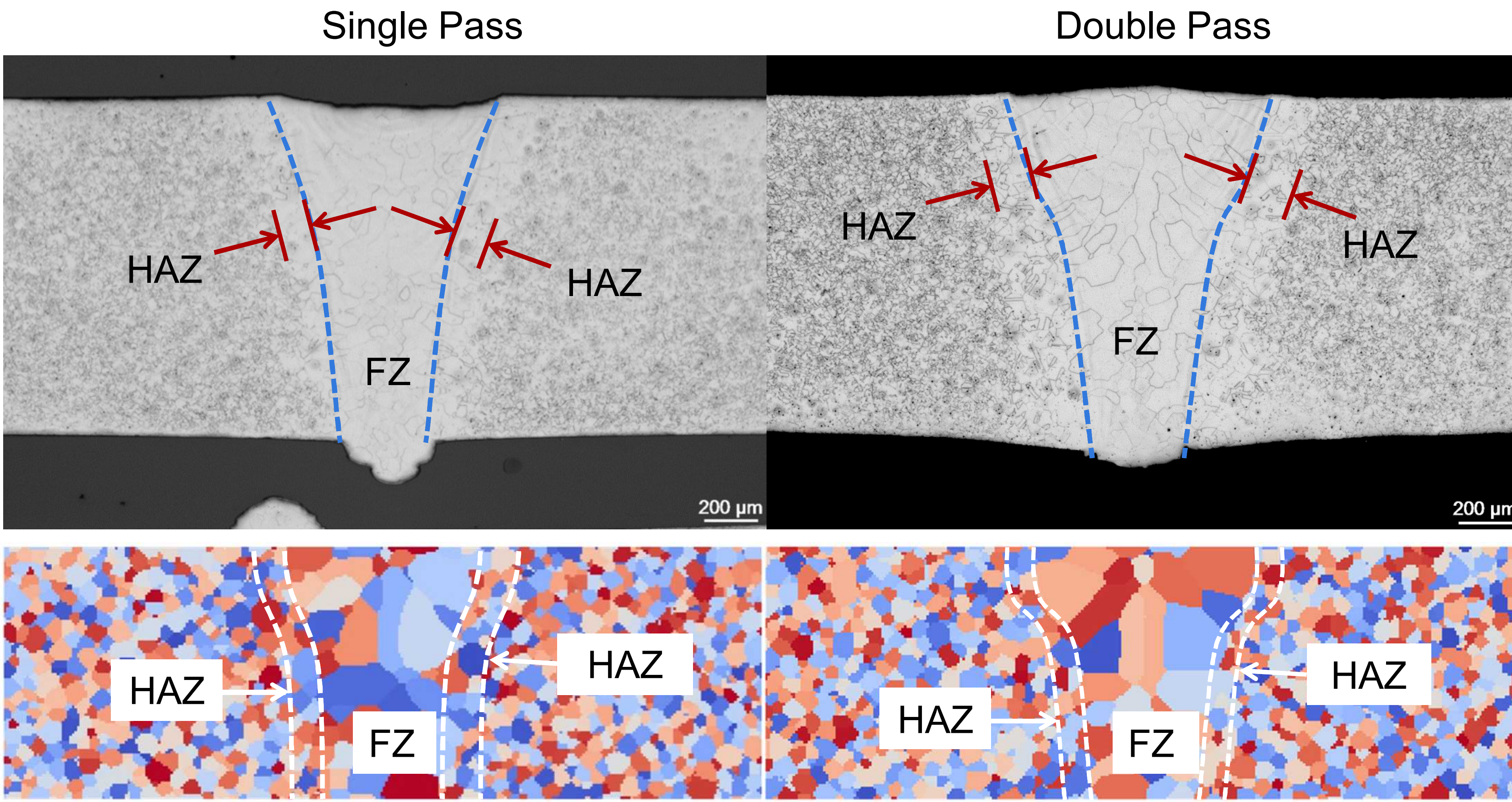

Rodgers, et al., ***JOM 2016***

Application to welding

Rodgers et al., MSMSE 2017

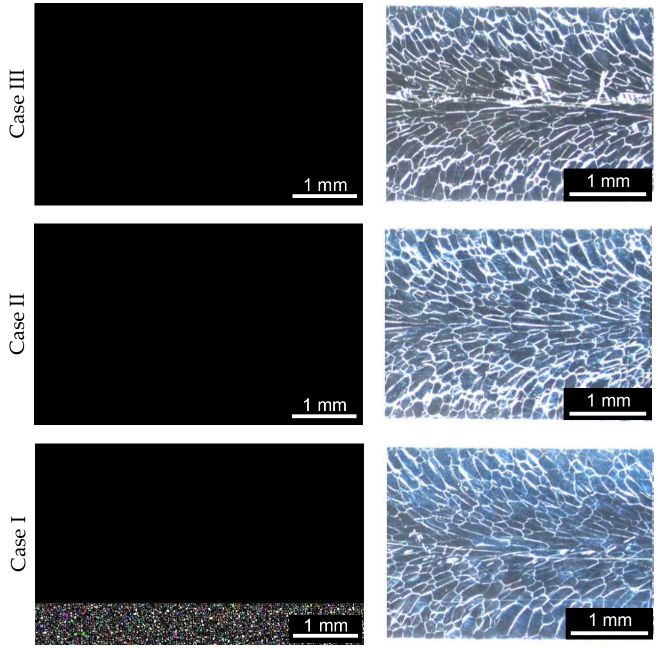

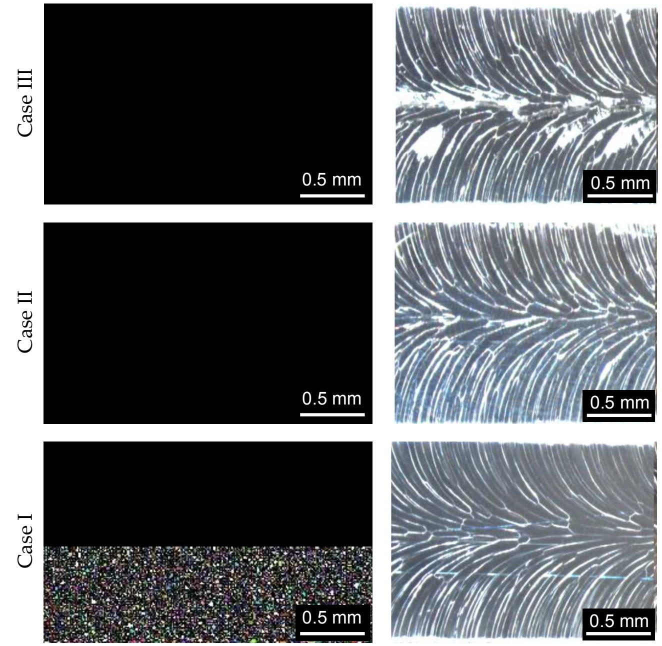

Rodgers et al., JOM 2016

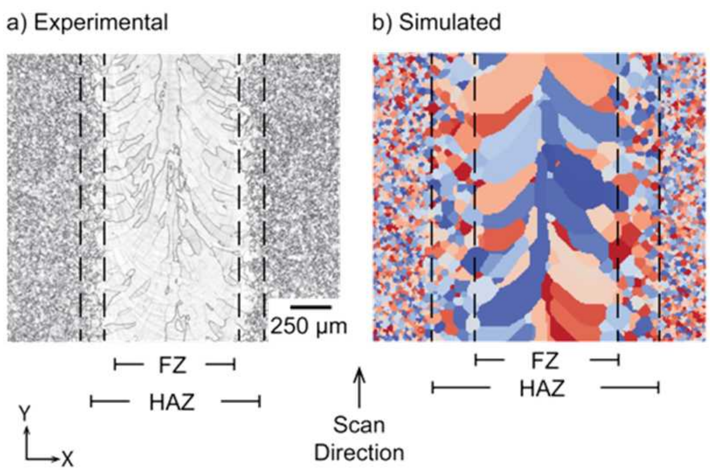

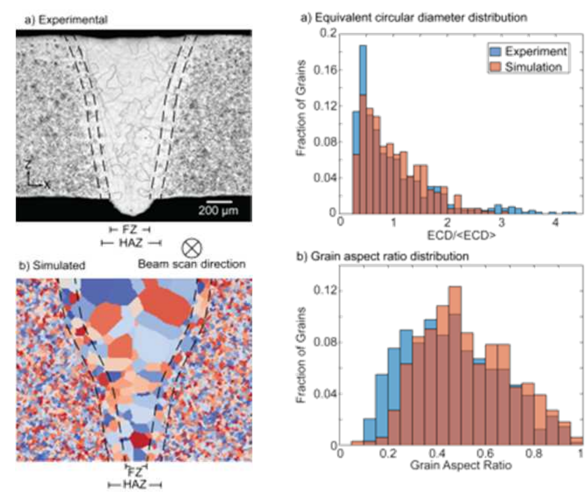

Outline

- Motivation
- Introduction to Monte Carlo-based microstructure modeling
- Application to solidification problems
  - Electron beam & laser welding
  - **Additive manufacturing**
- Using synthetic microstructures in further analysis
- Recent & on-going work

Columnar vs equiaxed microstructures

- Solidification grain morphology can be predicted through the ratio of temperature gradient (G) and solidification front velocity (R).
- For many melt pool geometries, G is smaller at the top (where curvature is lowest) and larger at the bottom. Resulting in smaller, equiaxed grains at the top and larger, columnar grains at the bottom.

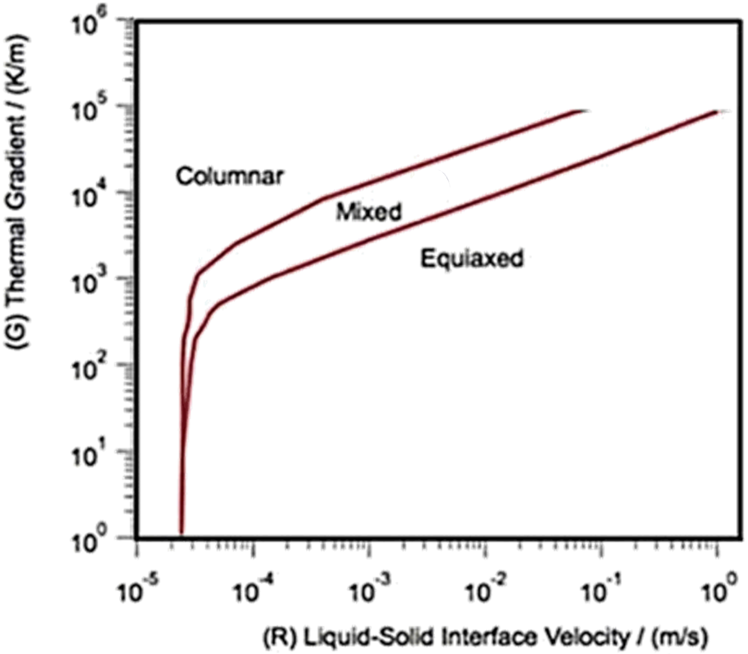

Wei et al., ***Proceedings of ReX&GG 2016***

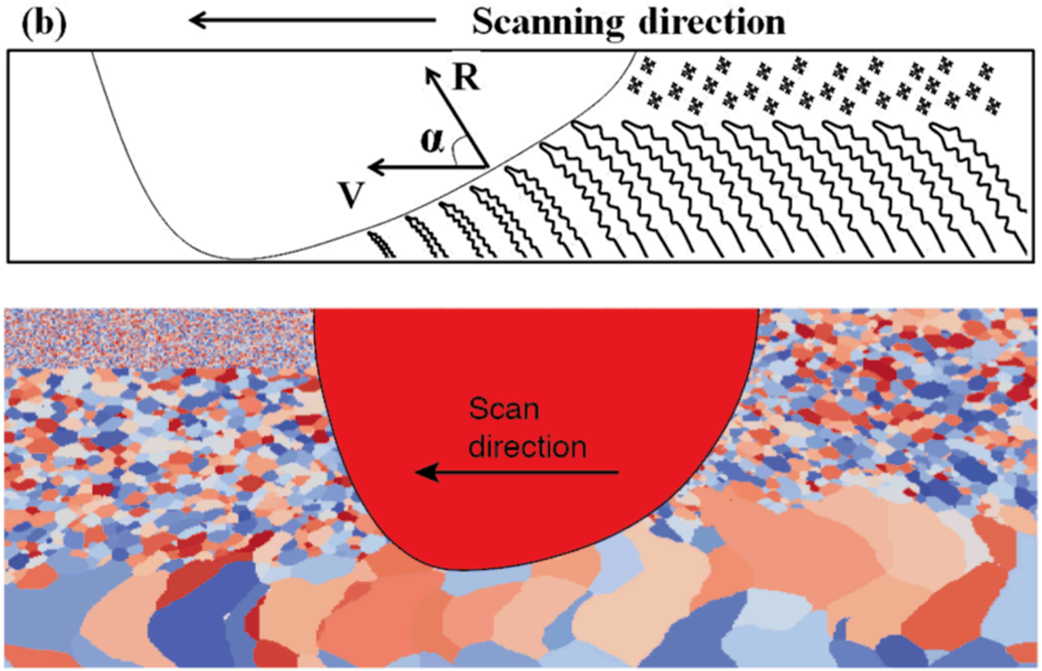

Application to various processes:

- Thin Wall Builds of Inconel 718 by DED

(Parimi et al., **Mater. Charact. 2014**)

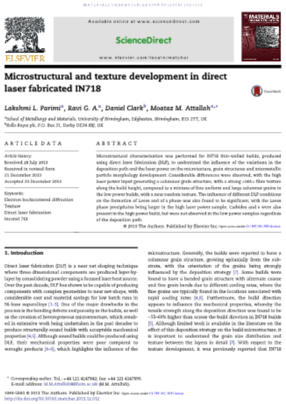
ScienceDirect

Microstructural and texture development in direct laser fabricated IN718

Lakshmi L. Parimi, Ravi G. A., Daniel Clark, Moataz M. Attallah

- Two-pass build of Ti-6V-4Al by Electron Beam Melting

(A. Antonysamy et al., **Mater. Charact. 2013**)

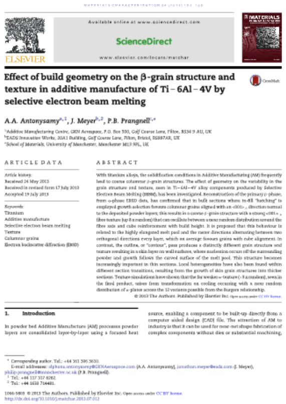
ScienceDirect

Effect of build geometry on the β-grain structure and texture in additive manufacture of Ti−6Al−4V by selective electron beam melting

A.A. Antonysamy, J. Meyer, P.B. Prangnell

- High-power LENS build of 304L Stainless Steel

(Nishida et al., **Proc. of DYMAT 2015**)


Dynamic compressive response of wrought and additive manufactured 304L stainless steels

Thin Wall Build Comparison (In718)

Parimi et al. demonstrated microstructure variation in three thin wall builds of Inconel 718.

Builds 1 & 2 used similar heat source specifications, but varying scan patterns.

Build 3 used a much higher power, but identical scan pattern as Build 2

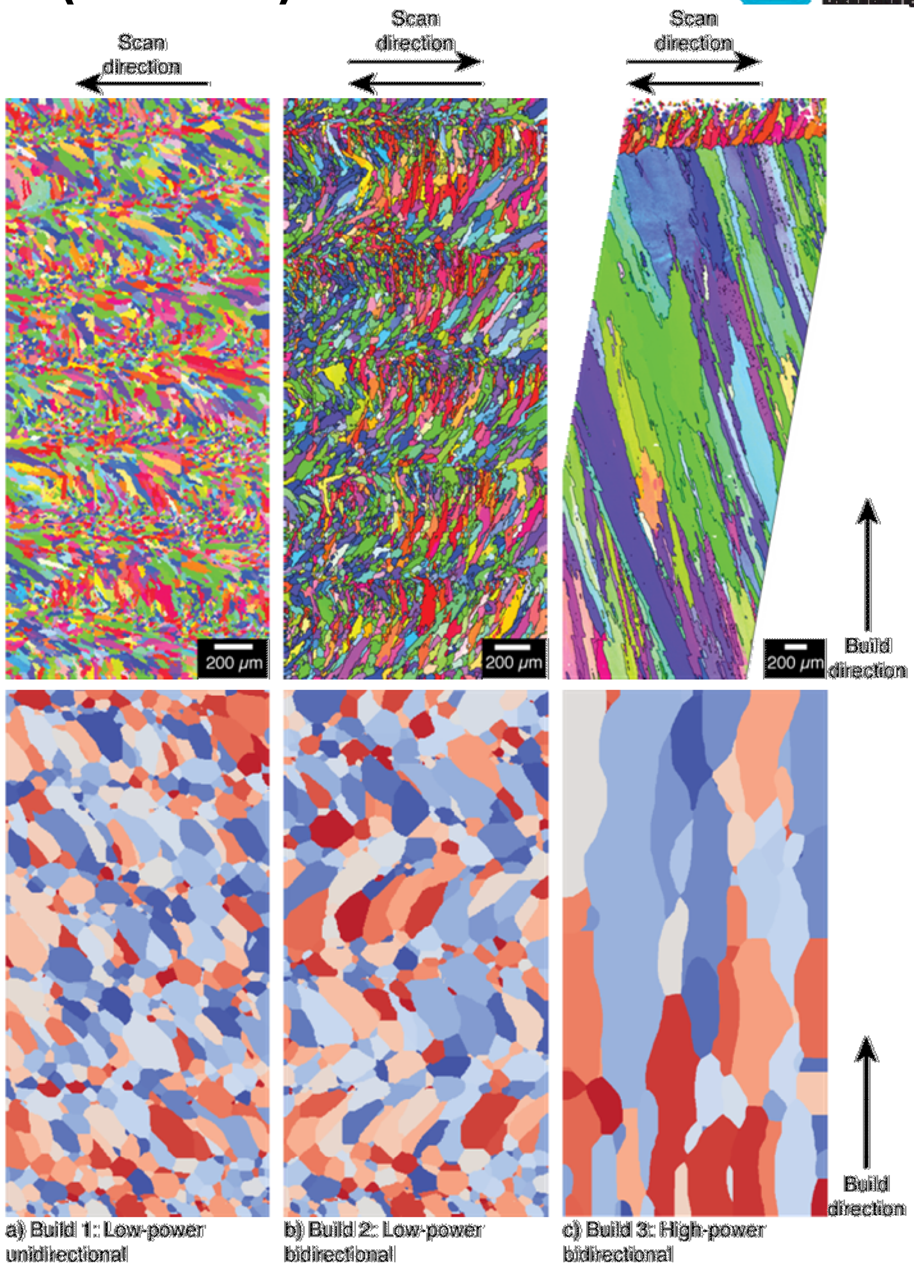

Thin Wall Build Quantitative Comparison

Dream.3D was used to measure grain tilt angles for the experimental and simulation images.

Simulated microstructures show similar trends in angle distribution, but with less scatter.

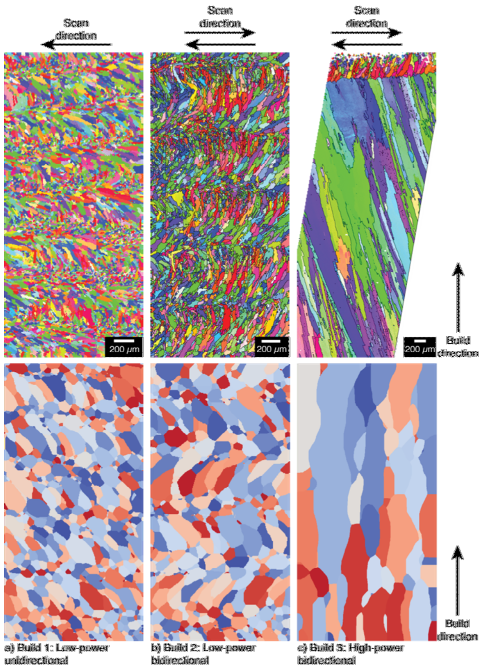

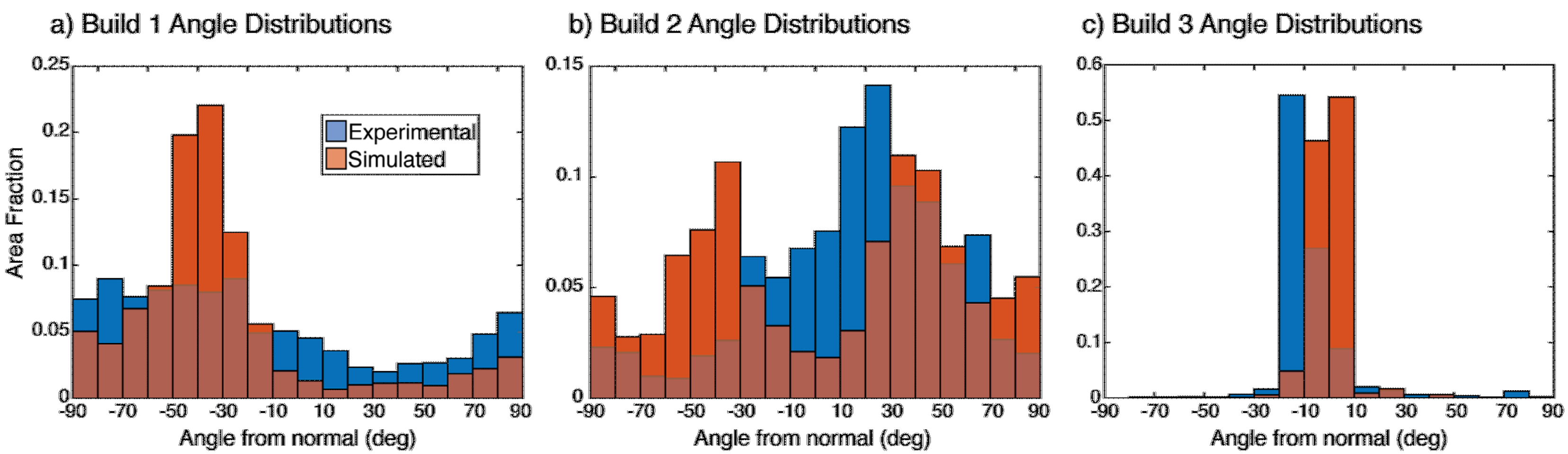

Parimi et al., ***Mater. Charact. 2014***

Two-pass quantitative comparison

Experimental and simulated microstructures were divided into three regions along the x-axis.

The central region had vertically aligned grains while either edge region had grains tilted towards the domain's centerline.

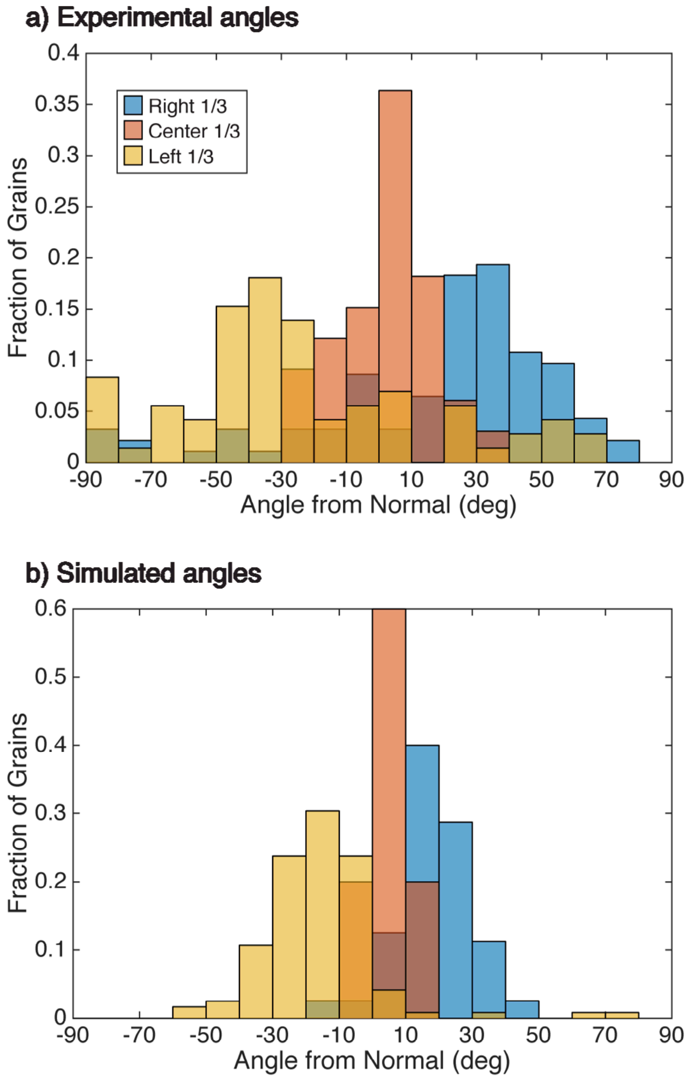

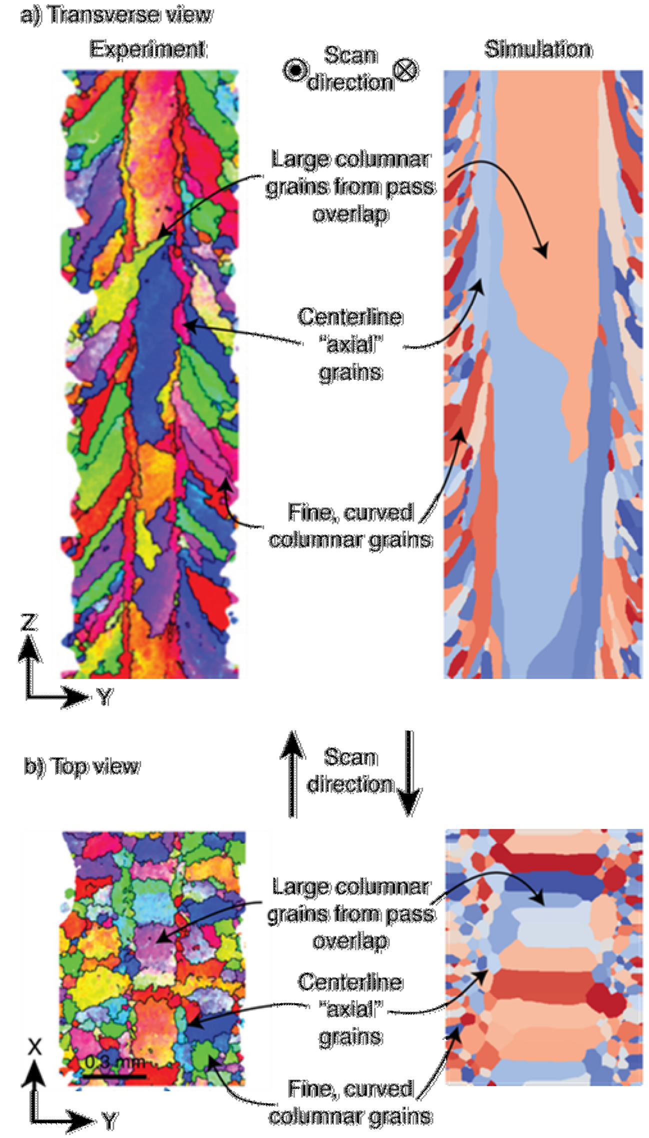

A. Antonysamy et al., ***Mater. Charact. 2013***

304L LENS Brick

Grain shape aspect ratios were measured along each of the three orthogonal planes.

Experimental and simulated distributions showed similar trends w.r.t. each plane, but simulation distributions remained narrower and more sharply peaked.

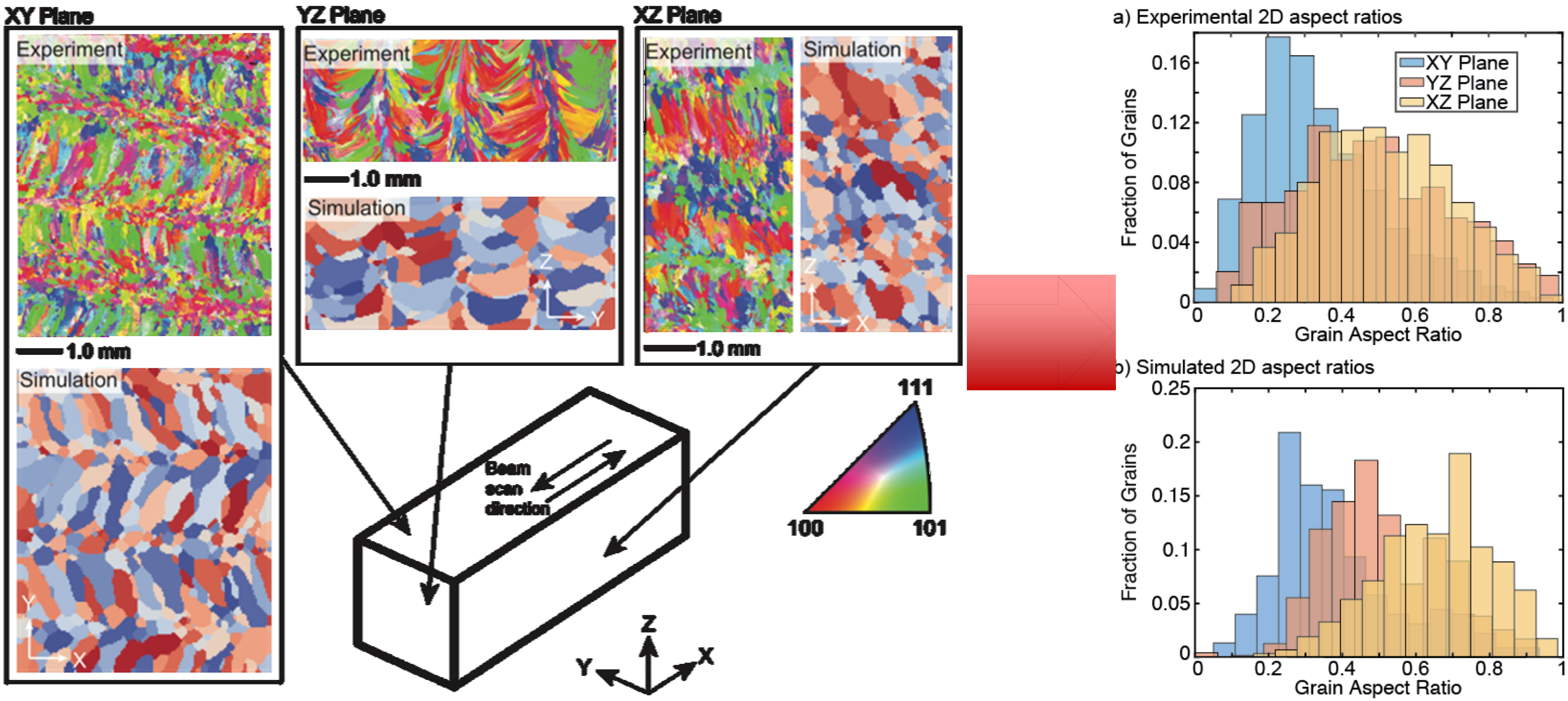

*Nishida et al., **Proc. Of DYMAT 2015***

Outline

- Motivation
- Introduction to Monte Carlo-based microstructure modeling
- Application to solidification problems
- **Using synthetic microstructures in further analysis**
  - Developing a data-driven reduced order microstructure prediction model
  - Microstructure-aware mechanics simulations
- Recent & on-going work

Workflow to extract Process-Structure Linkage

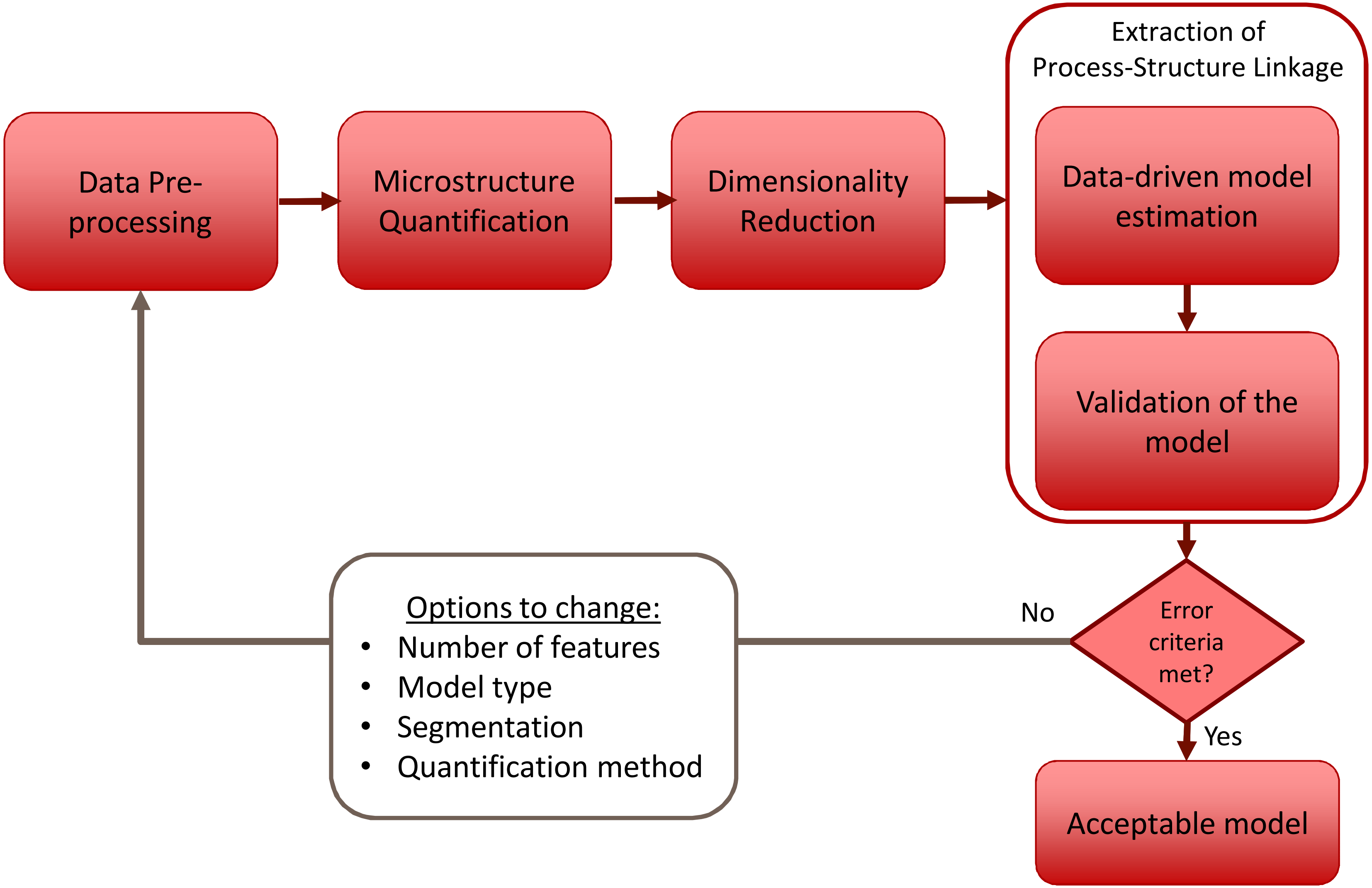

Microstructure Quantification: Chord Length Distribution (CLD)

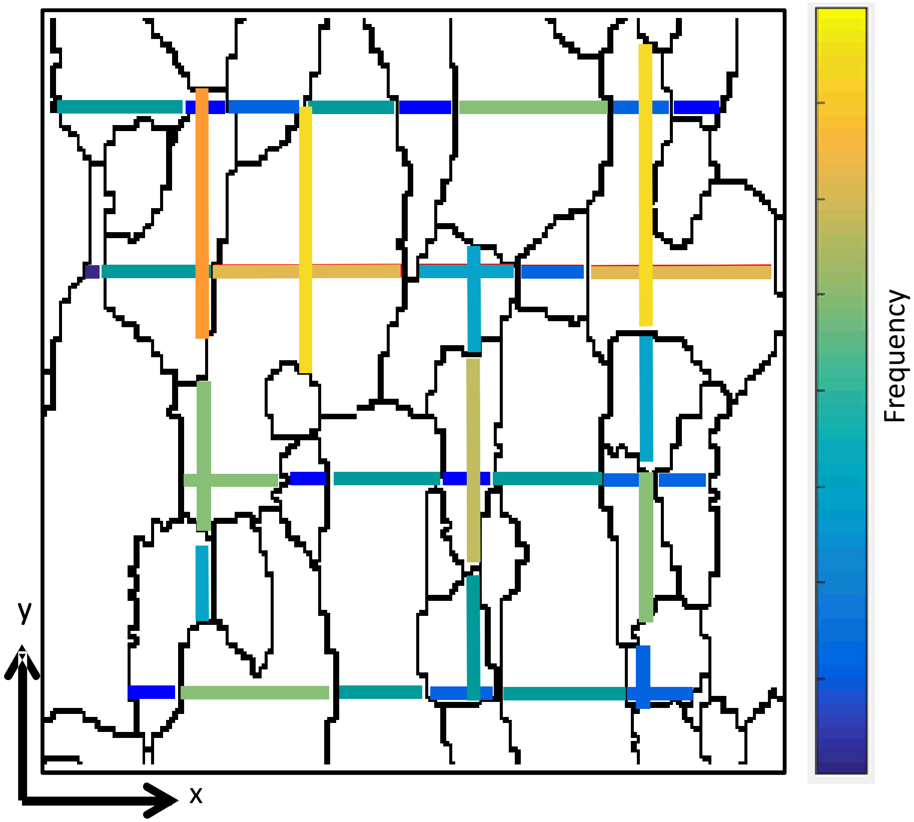

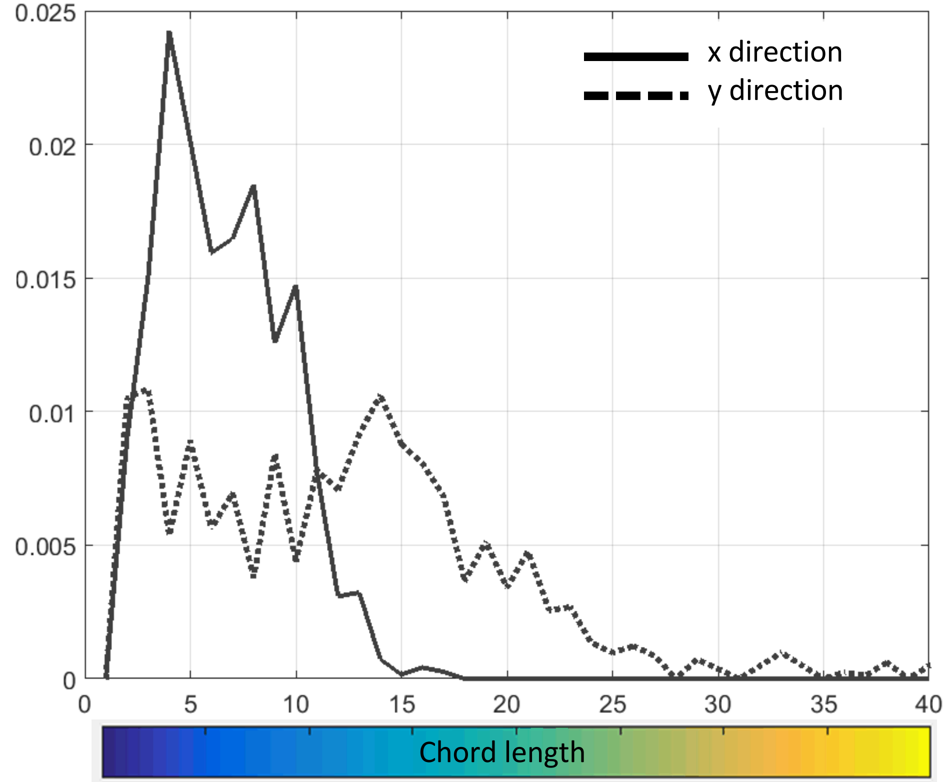

Popova, Rodgers, et al., ***IMMI 2017***

Chord Length Distribution (CLD)

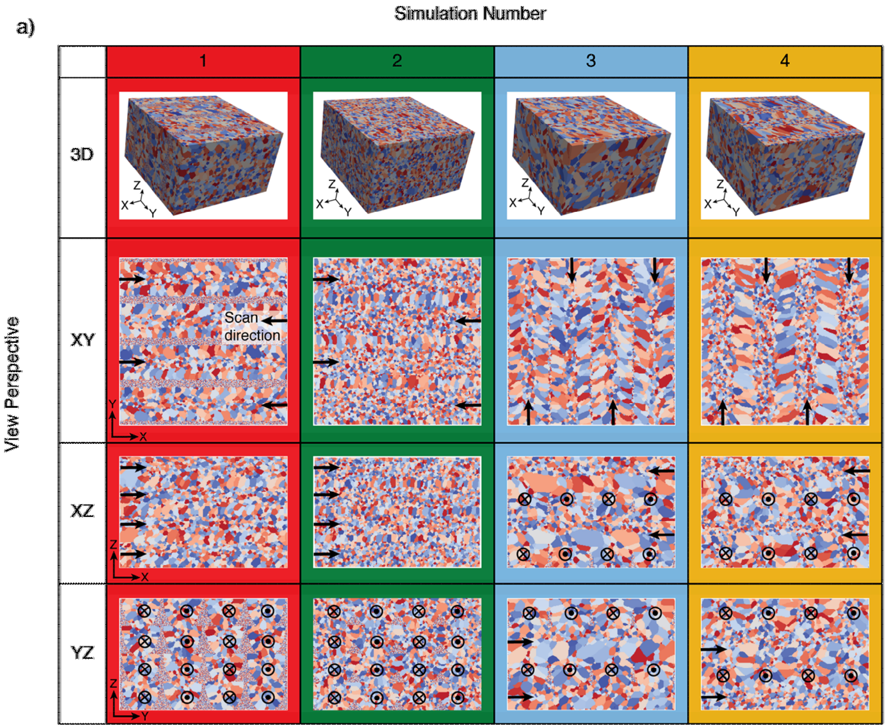

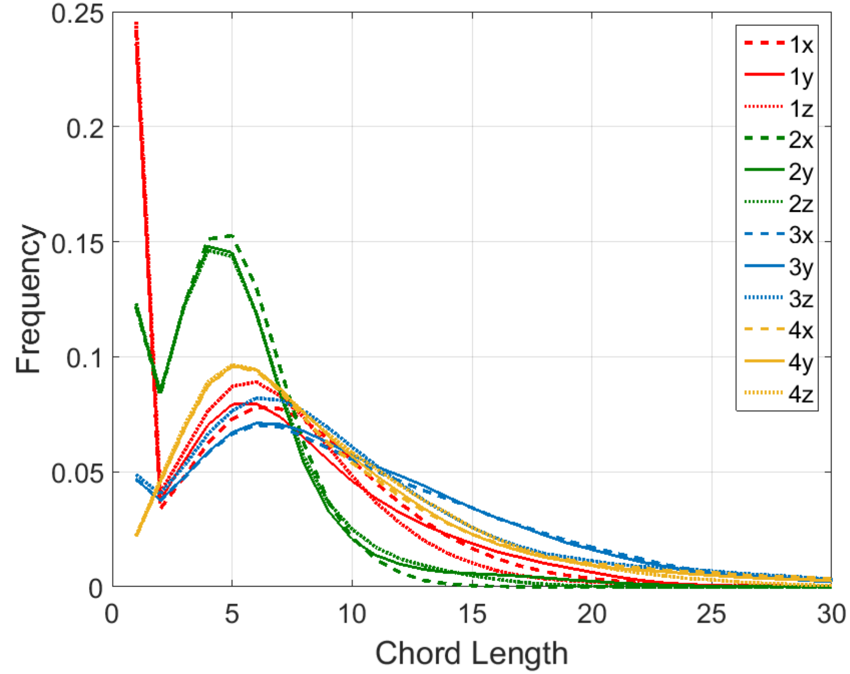

b)

Simulation Number

Parameter	1	2	3	4
X/XY	X	X	XY	XY
W	60	80	70	90
V	5	15	5	7.5
D	50	50	62.5	62.5
L	50	60	60	70
HAZ	5	5	20	35
T	5	20	20	35

- CLDs calculated in X,Y and Z directions
- After calculating CLD for all structures, the feature vector is 800 long
- The final data matrix is **1599x800** matrix

Popova, Rodgers, et al., ***IMMI 2017***

Dimensionality Reduction:
Principal Component Analysis (PCA)

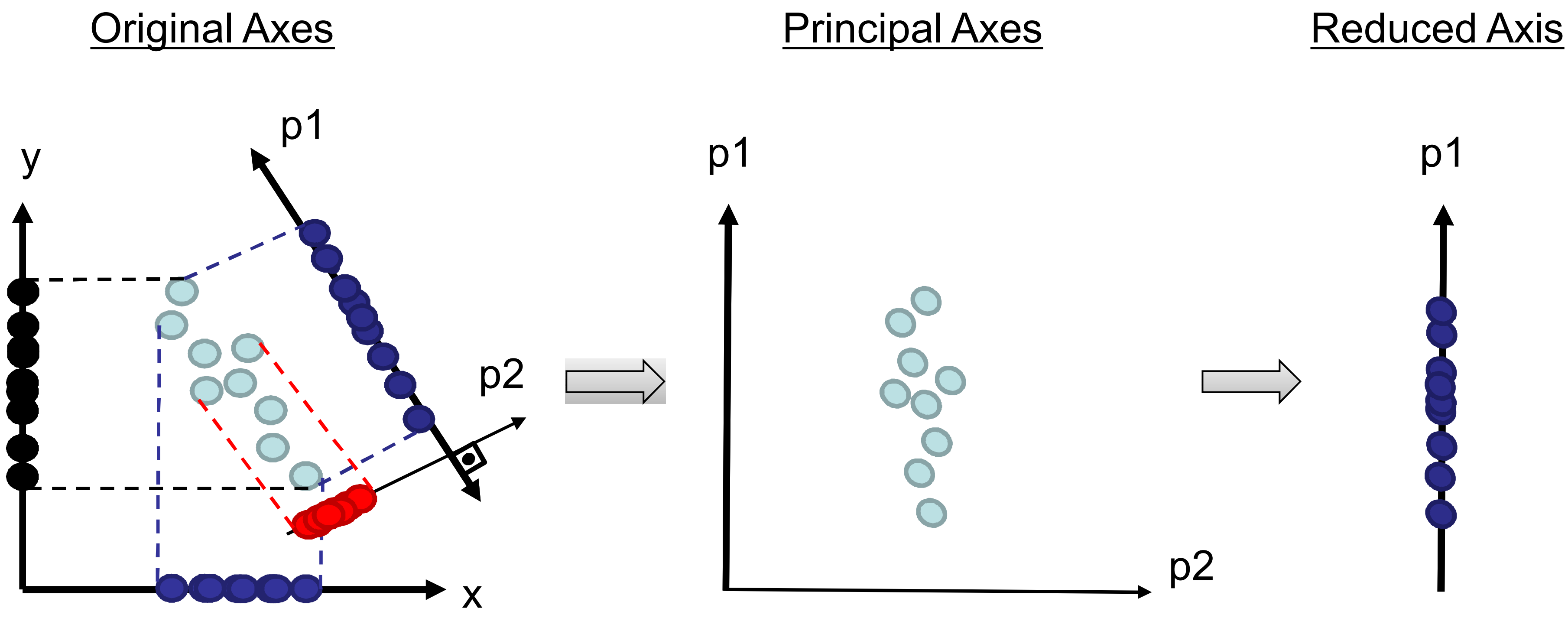

Principal component analysis identifies the most objective (data-driven) rotational transformation that re-organizes the data in prioritized directions of maximum variance

Principal Component Analysis (PCA)

$$CLD_m \approx \sum_{j}^{N} \alpha_j^m A_j + A_0$$

A_j - j^{th} principal component (each A_j is a vector of 800 statistics),
A_0 - mean CLD of all the microstructures in the dataset (also a vector of 800 statistics),
α_j^m - j^{th} PC score (for the microstructure indexed by *m*).
N - the truncation level selected based on the variance captured by the principal components

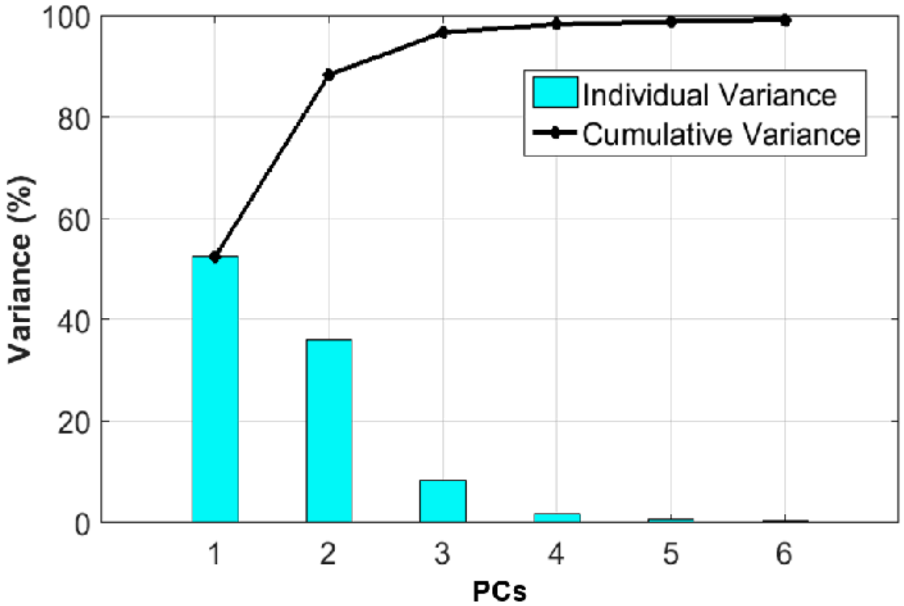

- PCA performed on concatenated CLDs
- over 98% variance captured by first 4 PCs

Popova, Rodgers, et al., ***IMMI 2017***

PCA of Chord Length Distributions

- Each point – CLD of one structure's

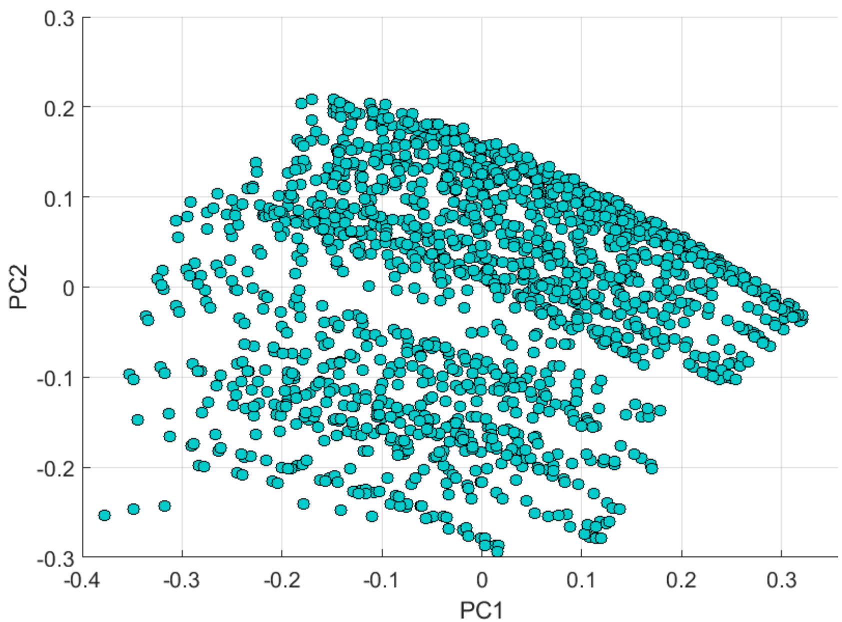

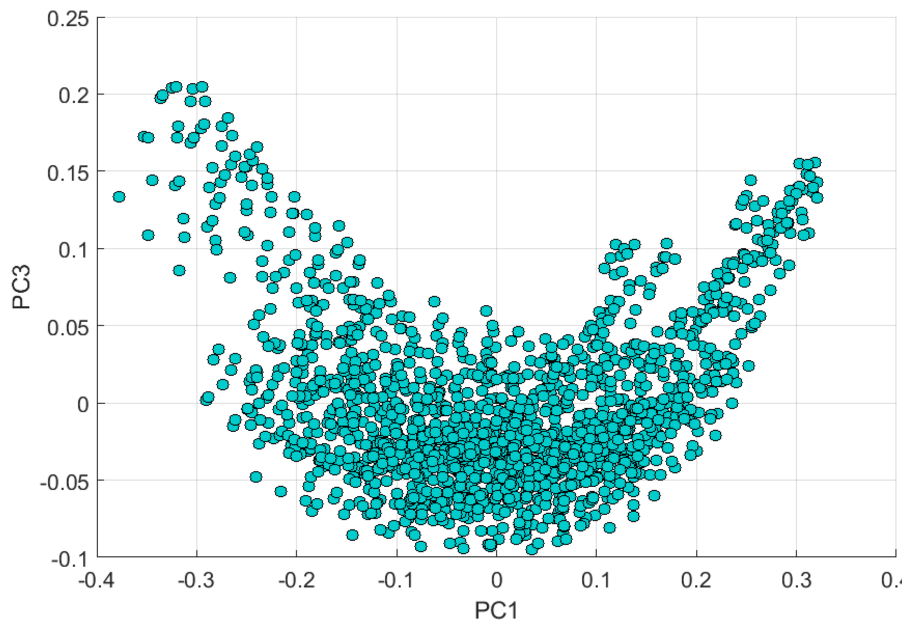

Popova, Rodgers, et al., ***IMMI 2017***

Extraction of PS Linkage: Model Selection and Validation

Full Dataset
1599
Microstructures

Establish Process Structure Linkage through a Metamodel Learned via Regression

$$\alpha_j = f_j(T, V, W, D, L, HAZ)$$

Principal Components as a Function of Process Parameters

Use the Newly Established Linkage to Predict the Structure of New Data, Given Only Process Parameters

Evaluate the Performance of the Linkage

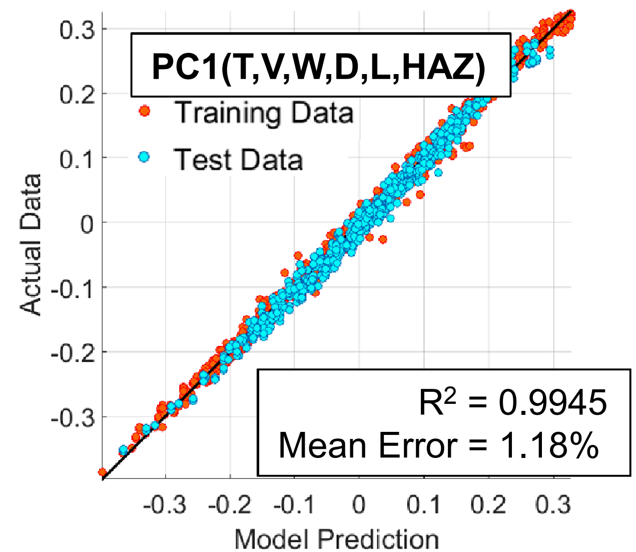

For Each Principal Component

Validation of the model with Test set

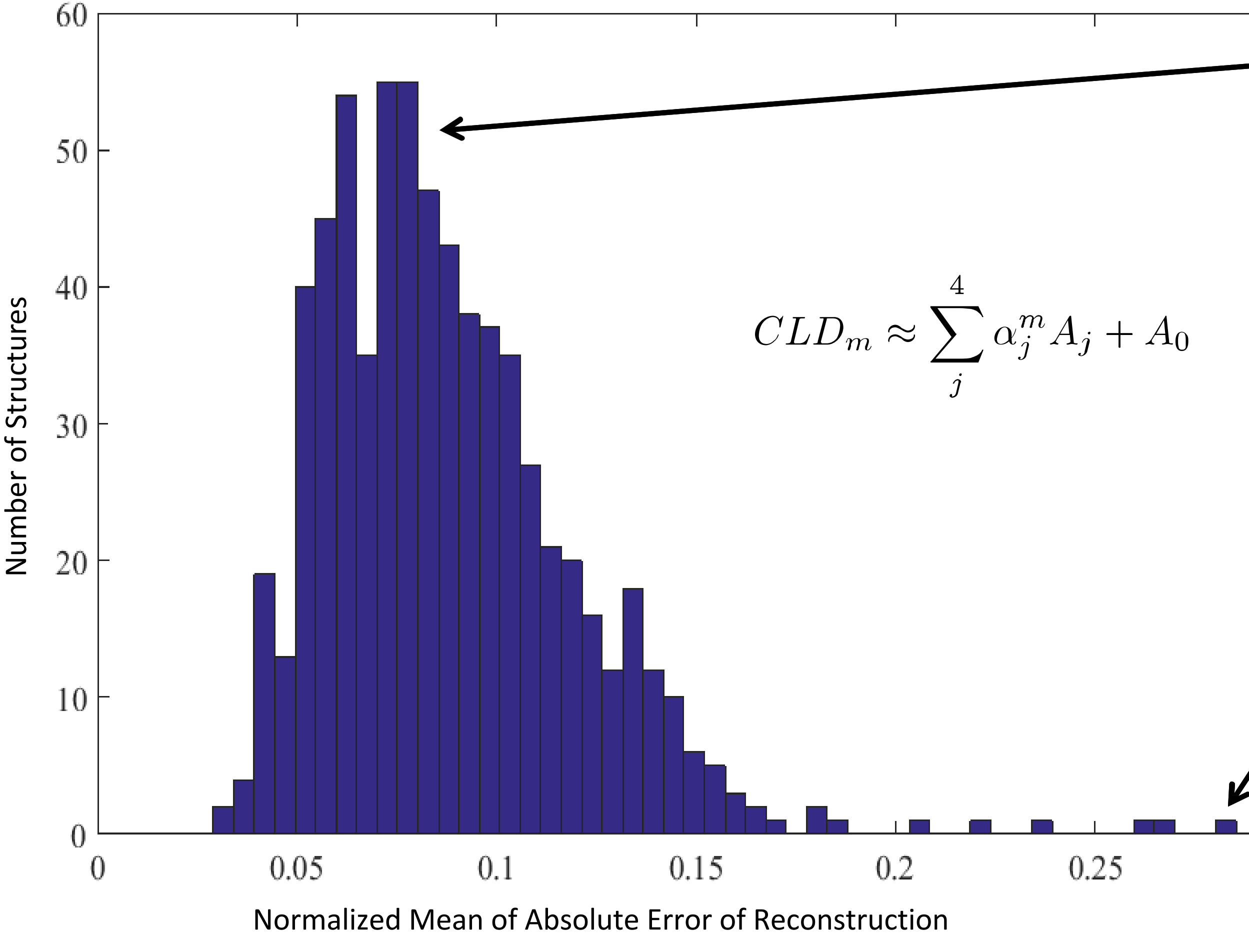

$$CLD_m \approx \sum_{j}^{4} \alpha_j^m A_j + A_0$$

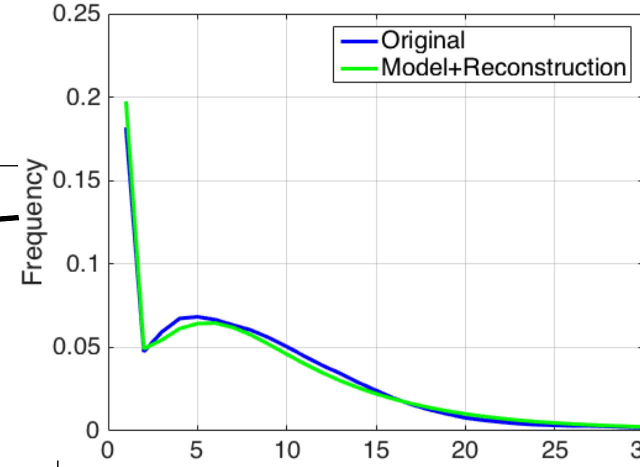

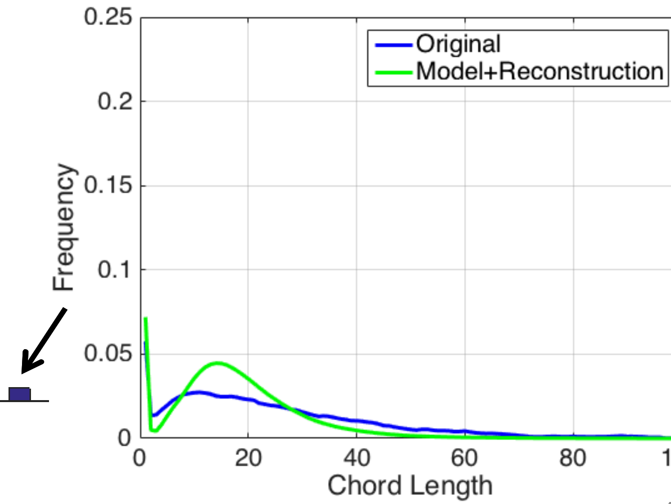

Outline

- Motivation
- Introduction to Monte Carlo-based microstructure modeling
- Application to solidification problems
- Using synthetic microstructures in further analysis
  - Developing a data-driven reduced order microstructure prediction model
  - **Microstructure-aware mechanics simulations**
- Recent & on-going work

Using Synthetic Microstructures in Mechanics simulations

Additive simulations were performed at four scan velocities.

Scan patterns consisted of two concentric circular scans per layer.

Idealized molten pool was used again but with curvature along the scan path.

Microstructure variation occurred with changing scan velocities and at various locations in the wall thickness.

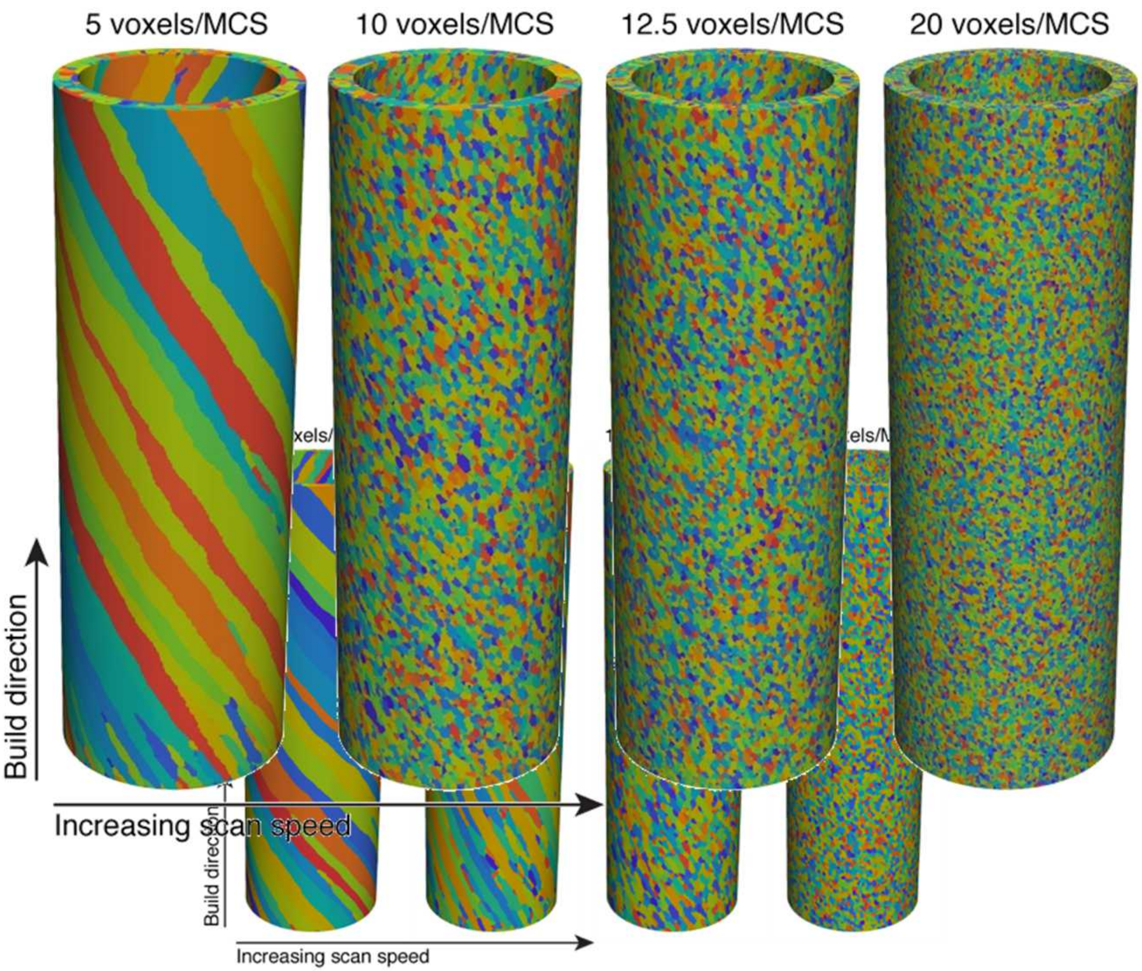

Rodgers, Bishop & Madison, Submitted to MSMSE

Interpolating from voxelized to conformal mesh

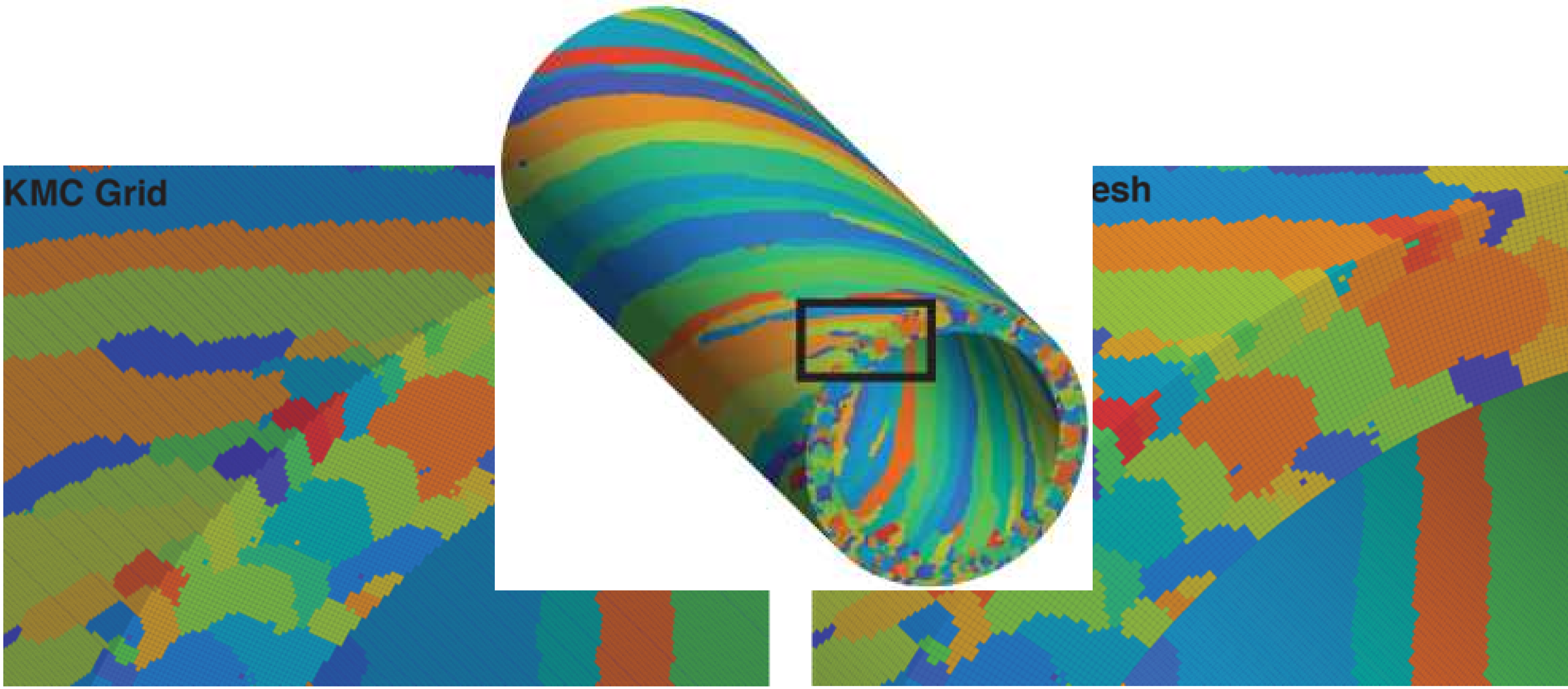

Rodgers, Bishop & Madison, Submitted to MSMSE

Stress response under tension

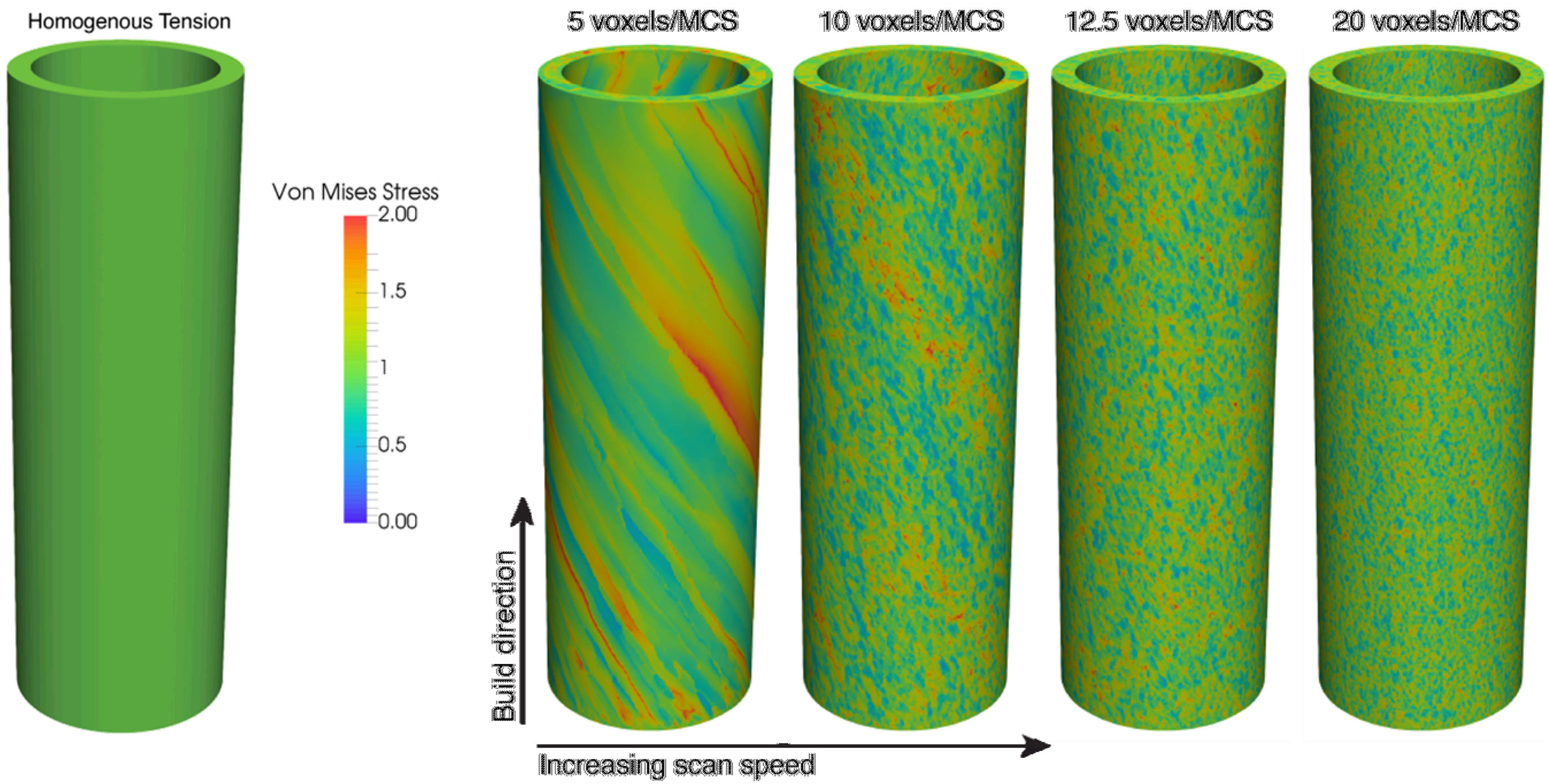

Rodgers, Bishop & Madison, Submitted to MSMSE

Stress response under tension

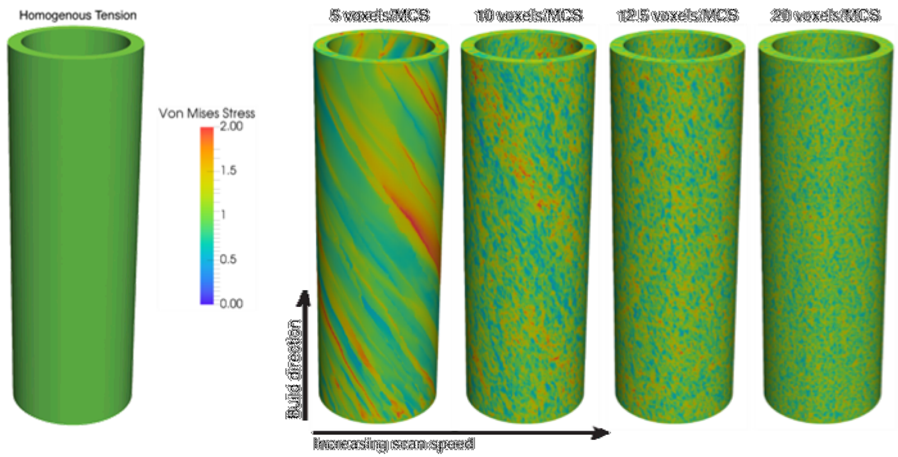

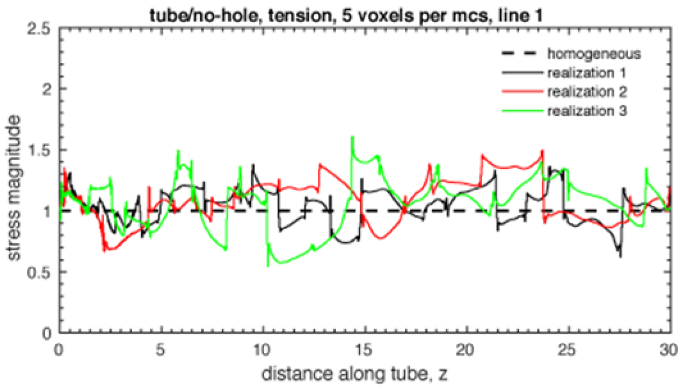

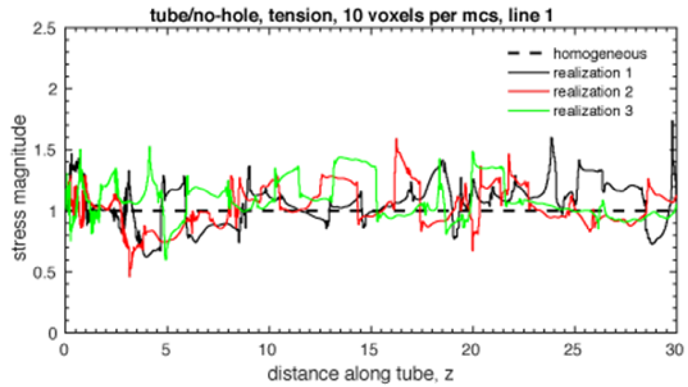

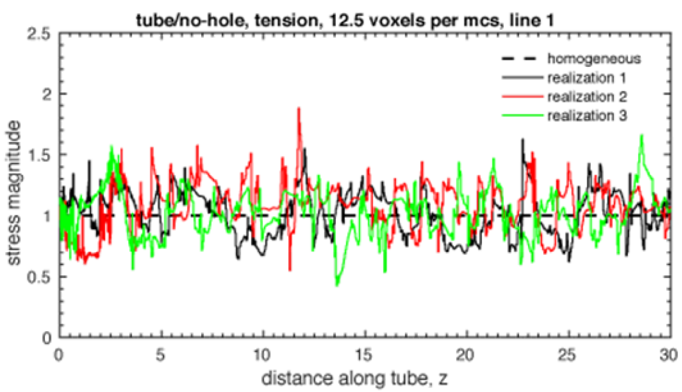

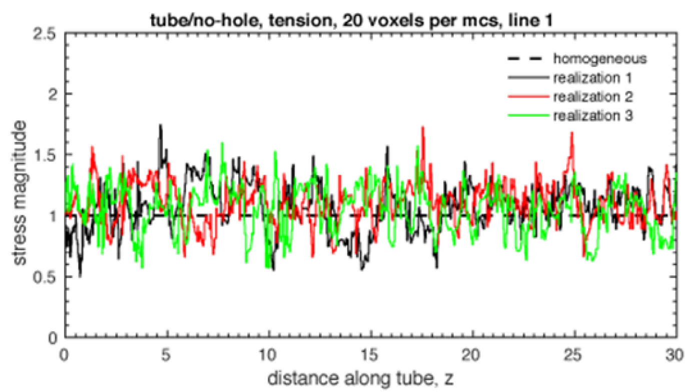

Rodgers, Bishop & Madison, Submitted to MSMSE

Stress response under torsion

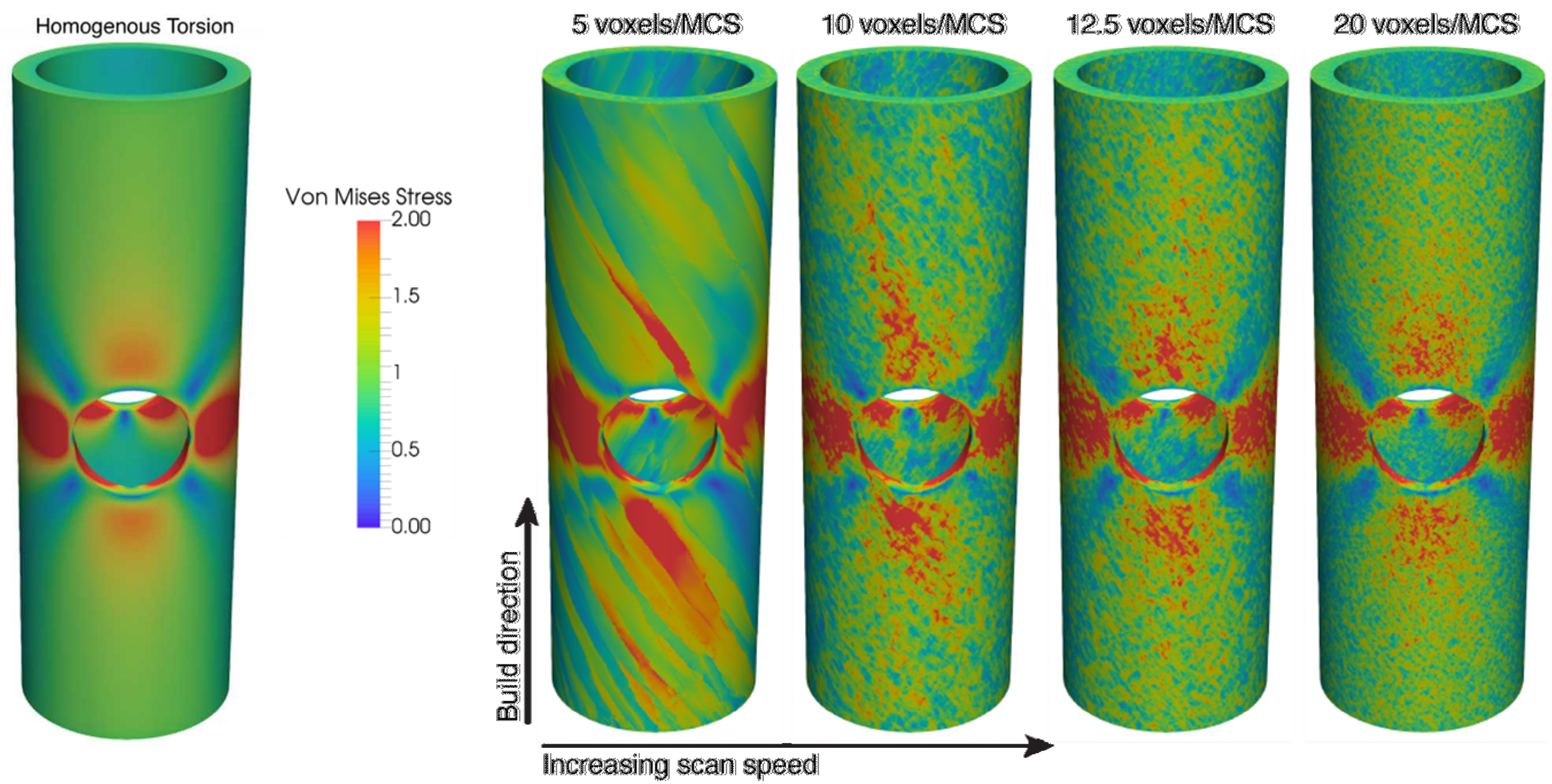

Rodgers, Bishop & Madison, Submitted to MSMSE

Stress response under torsion

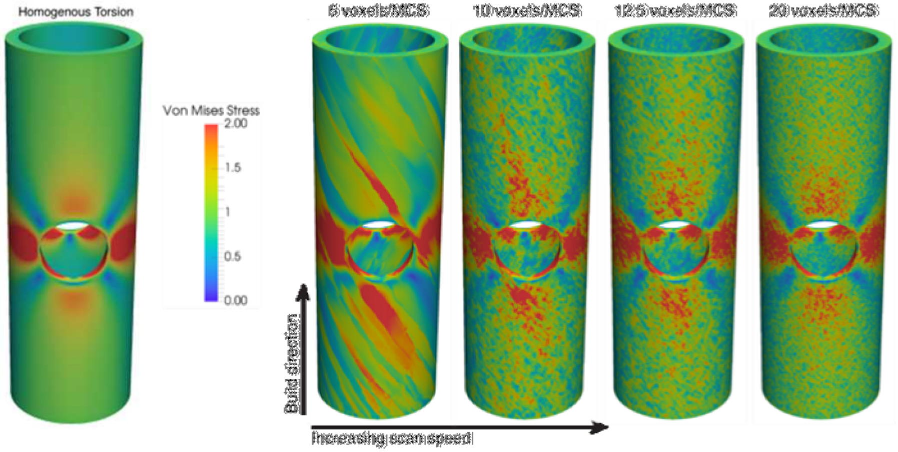

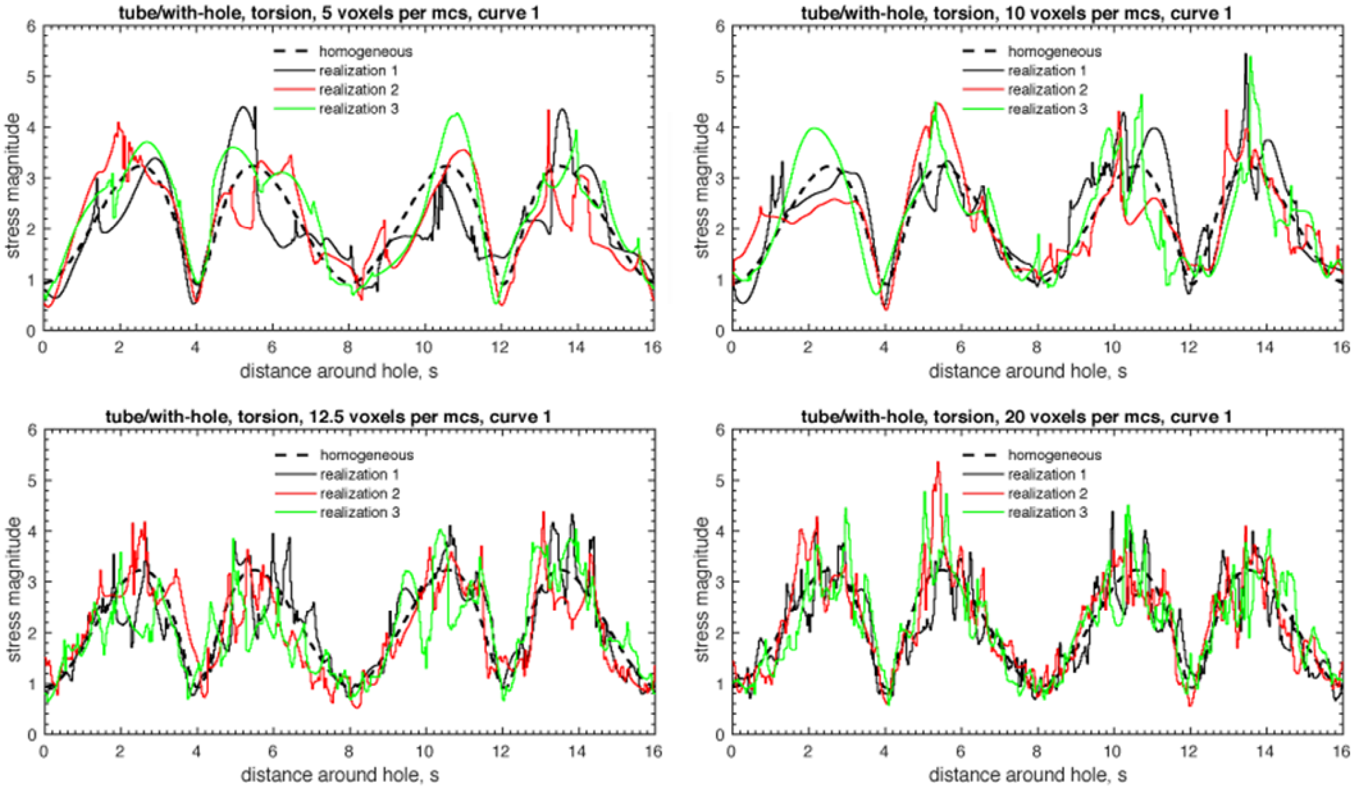

Rodgers, Bishop & Madison, Submitted to MSMSE

Outline

- Motivation
- Introduction to Monte Carlo-based microstructure modeling
- Application to solidification problems
- Using synthetic microstructures in further analysis
- **Recent & on-going work**
  - Utilizing thermal fields from finite element simulations
  - Texture evolution
  - Finite-difference based thermal diffusion model
  - Thermofluid model coupling

304L Tube Example

<u>Case 1</u>
No inter-layer delay
(continuous build)

<u>Case 2</u>
8 second delay added
between layers
(double build)

Can we capture the difference in microstructure and residual stress due to changing thermal gradients?

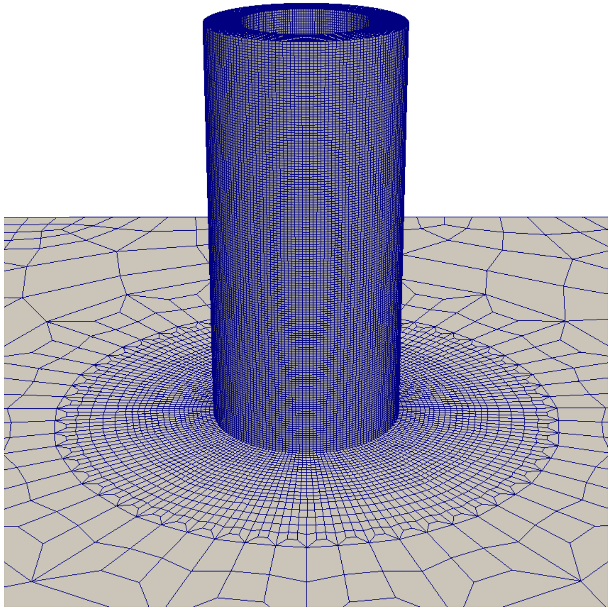

- LENS process
- Laser diameter = 4 mm
- Laser Speed = 8.46 mm/s
- Layer Thickness = 0.9 mm
- Laser Power = 2000 > 1750 > 1500 > 1250 W

Johnson, Rodgers et al, ***JCM 2017***

Thermal Comparison

Single Build

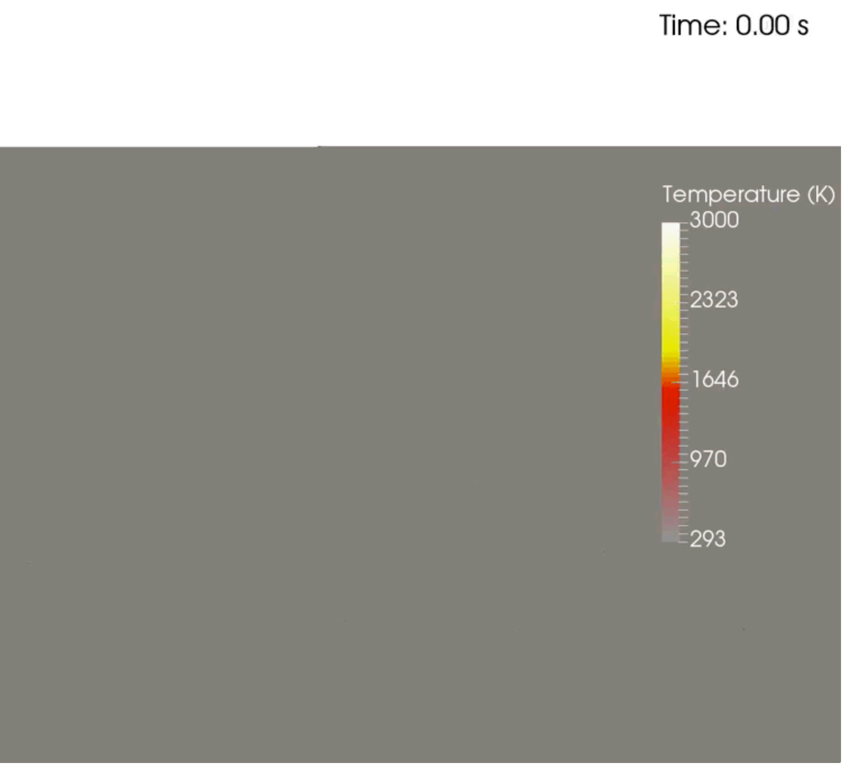

Double Build – 8 Second Inter-layer Delay

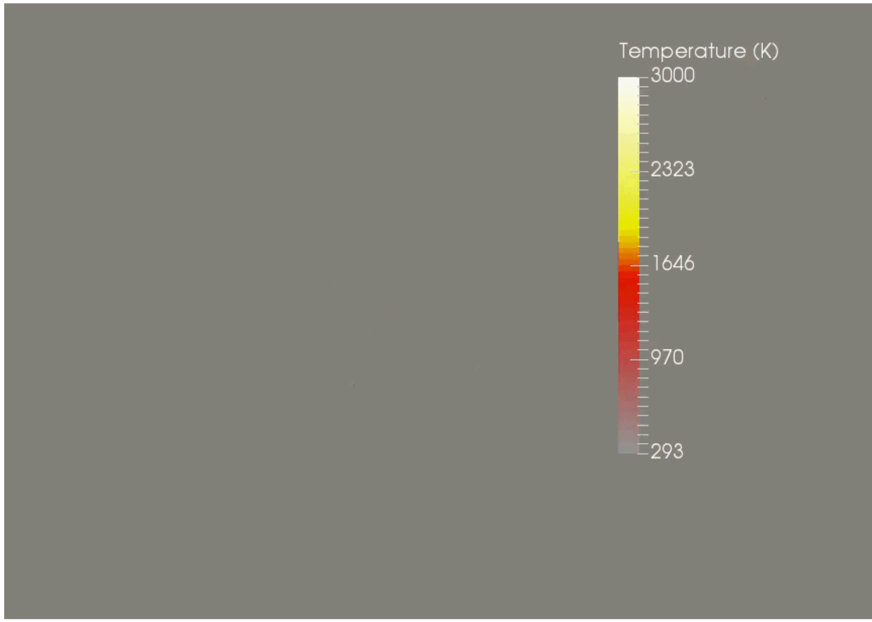

*Johnson, Rodgers et al, **JCM 2017***

Delay Time Lowers Global Part Temperature

Single Build

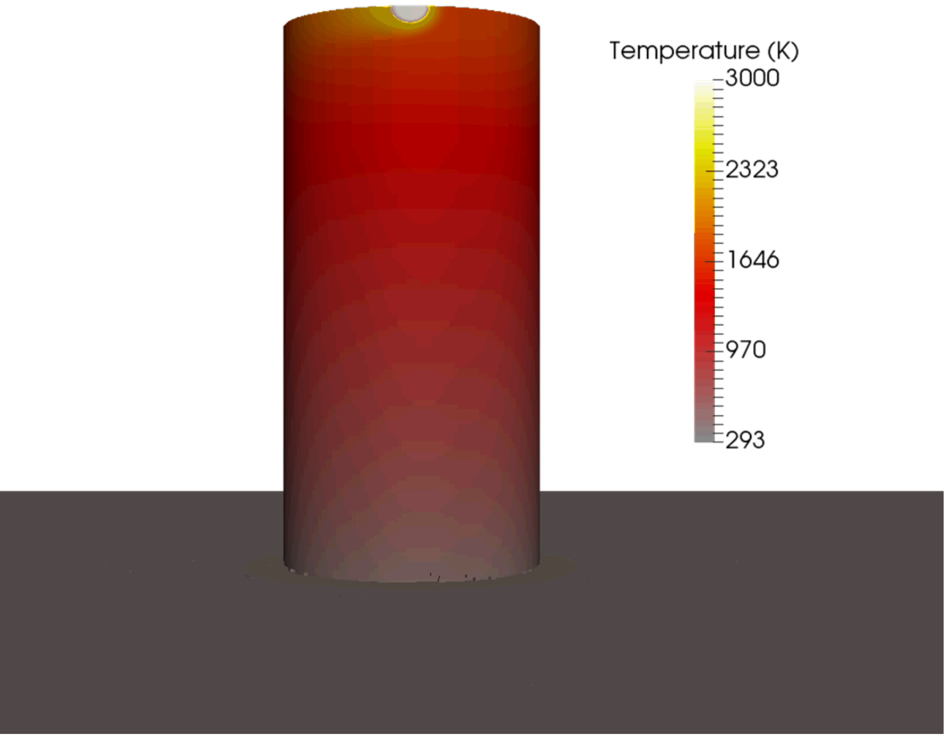

Double Build – 8 Second Inter-layer Delay

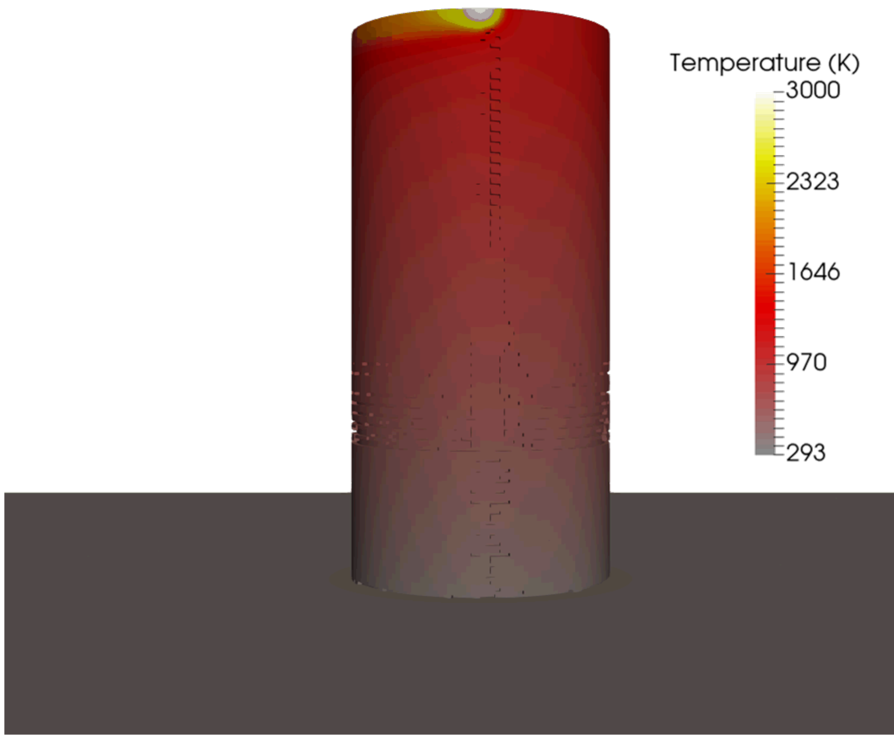

Johnson, Rodgers et al, ***JCM 2017***

Residual Stress Comparison

Single Build

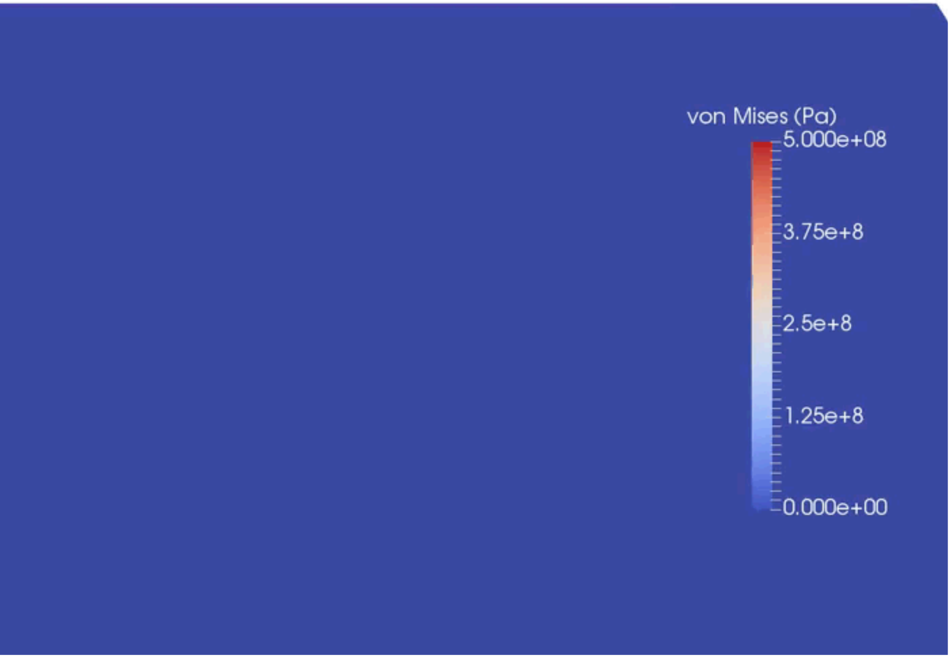

Double Build – 8 Second Inter-layer Delay

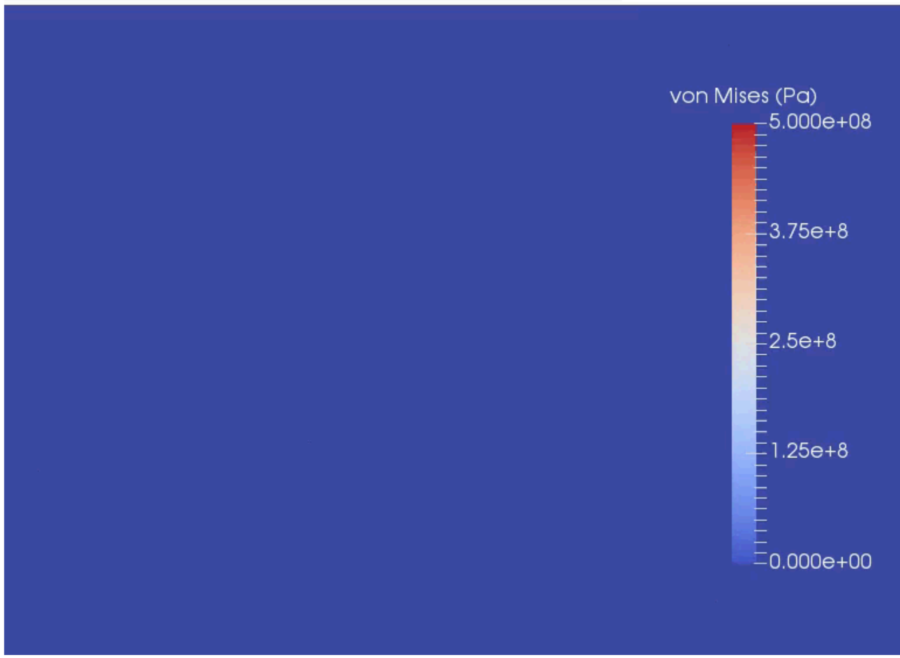

*Johnson, Rodgers et al, **JCM 2017***

Delay time causes lower overall von Mises stress

Single Build

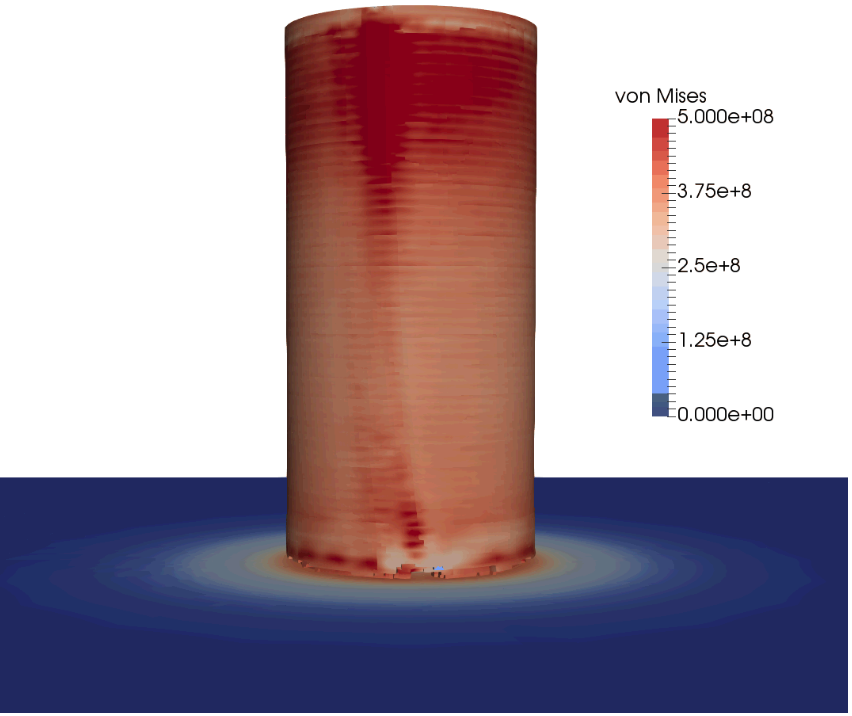

Double Build – 8 Second Inter-layer Delay

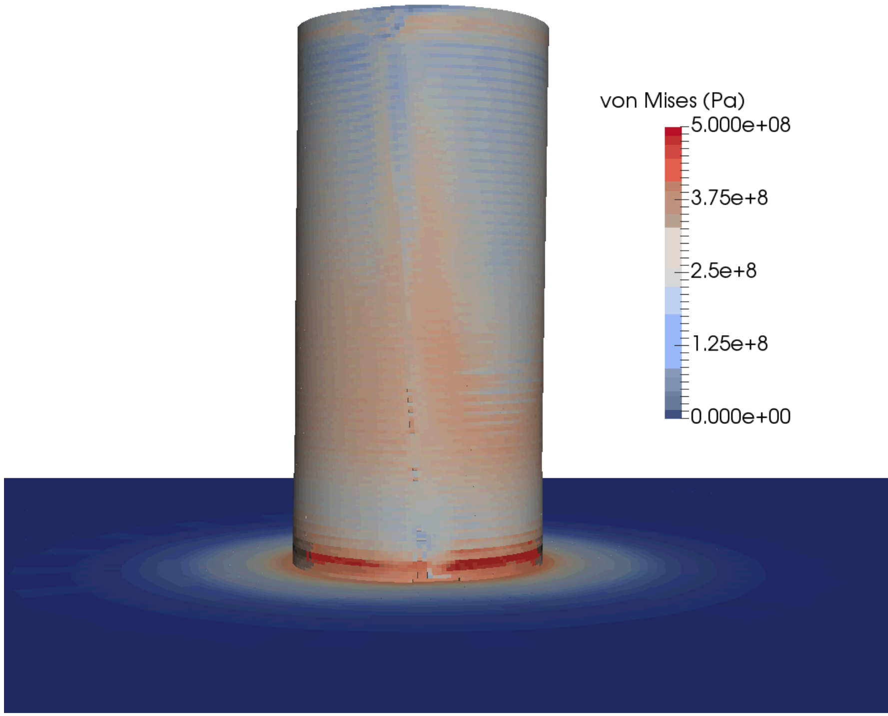

*Johnson, Rodgers et al, **JCM 2017***

Microstructure Comparison

Single Build

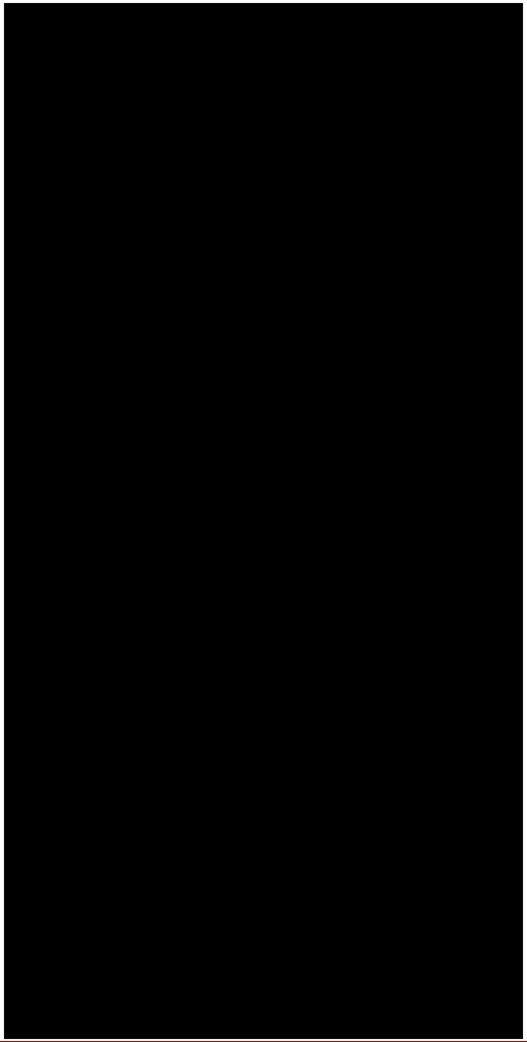

Double Build – 8 Second Inter-layer Delay

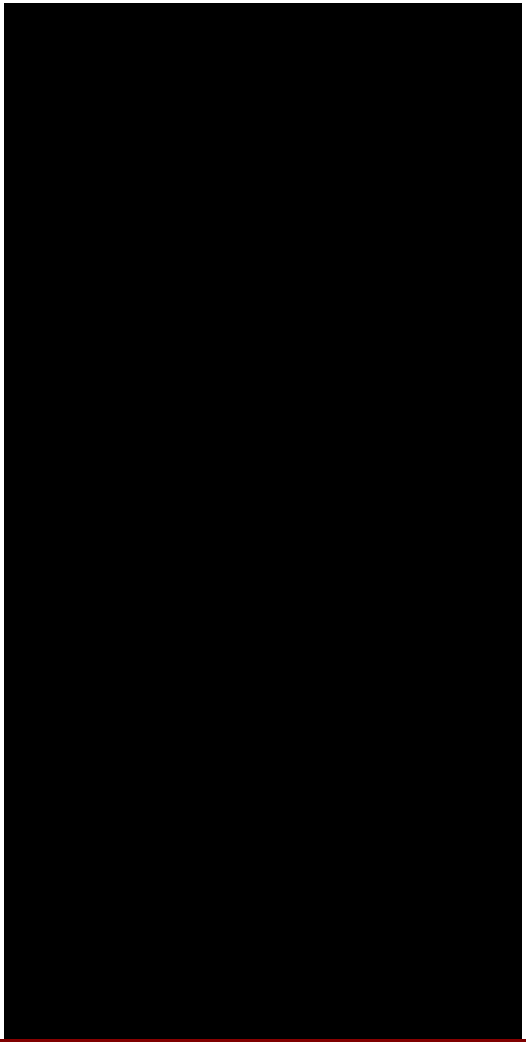

Johnson, Rodgers et al, ***JCM 2017***

Delay time inhibits equiaxed to columnar transition

Single Build

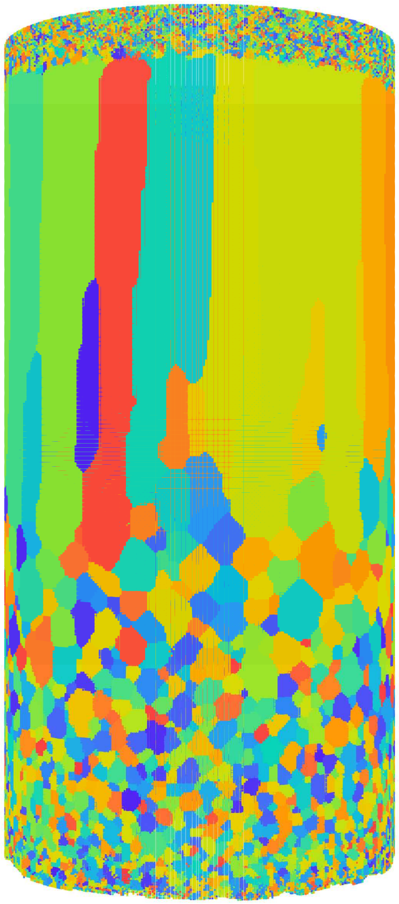

Double Build – 8 Second Inter-layer Delay

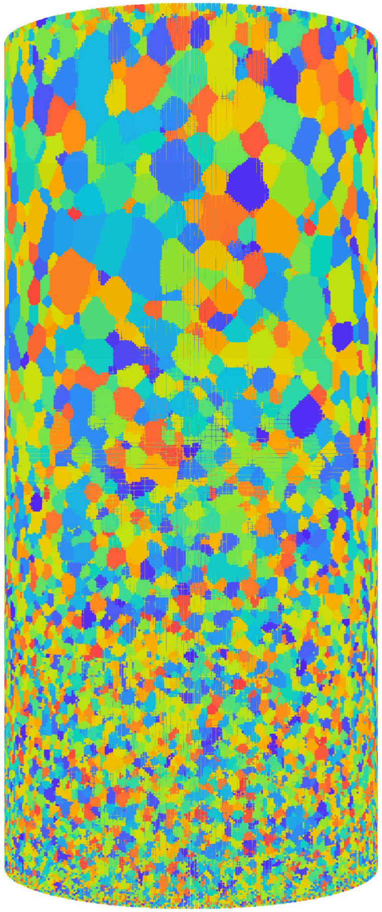

Johnson, Rodgers et al, ***JCM 2017***

Experimental Comparison - Microstructure

Experiment

Simulation

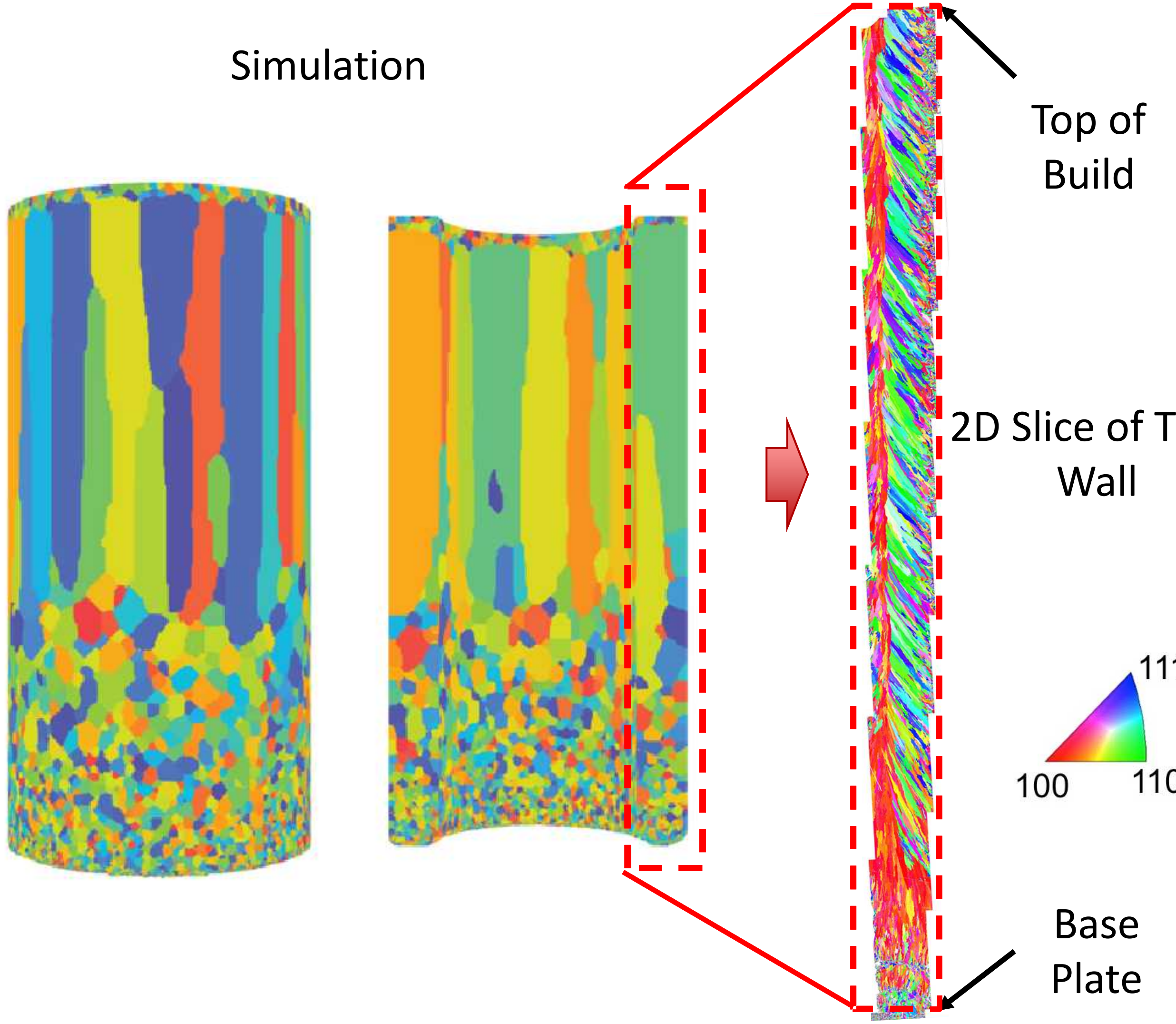

EBSD: O. Underwood, J. Madison, A. Kilgo, J. Michael, S. Dickens

Outline

- Motivation
- Introduction to Monte Carlo-based microstructure modeling
- Application to solidification problems
- Using synthetic microstructures in further analysis
- Recent & on-going work
  - Utilizing thermal fields from finite element simulations
  - **Texture evolution**
  - Finite-difference based thermal diffusion model
  - Thermofluid model coupling

Texture variation often coincides with grain morphology variation

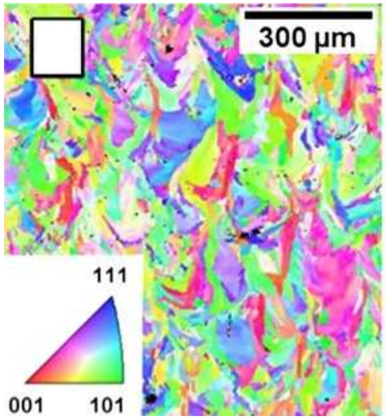

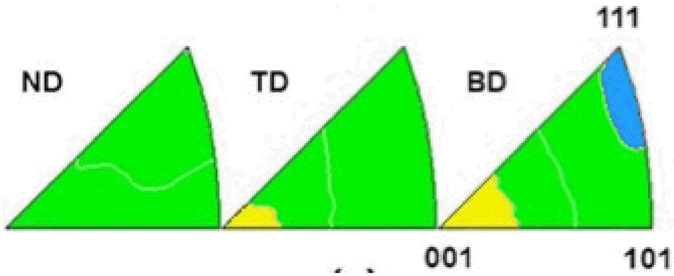

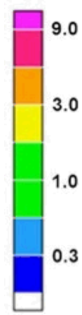

Niendorf et al., ***Metall. Mater. Trans. B 2013***

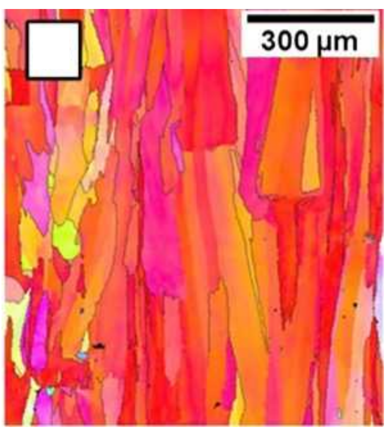

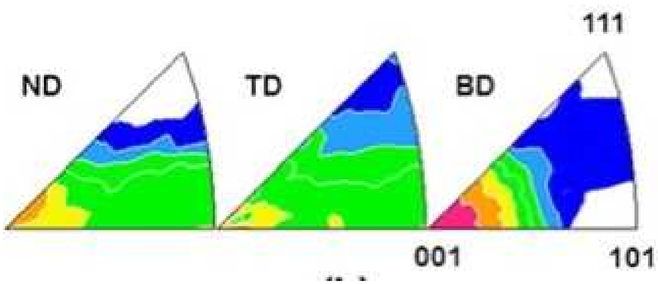

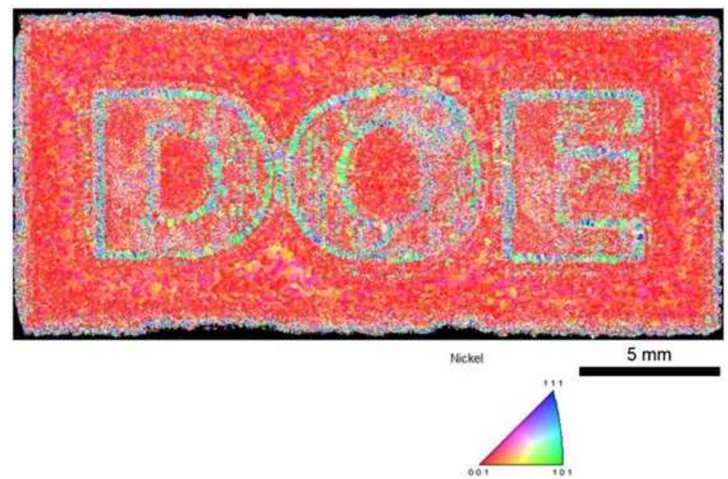

Dehoff et al., ***Materials Science and Technology 2015***

Select fast-solidifying directions

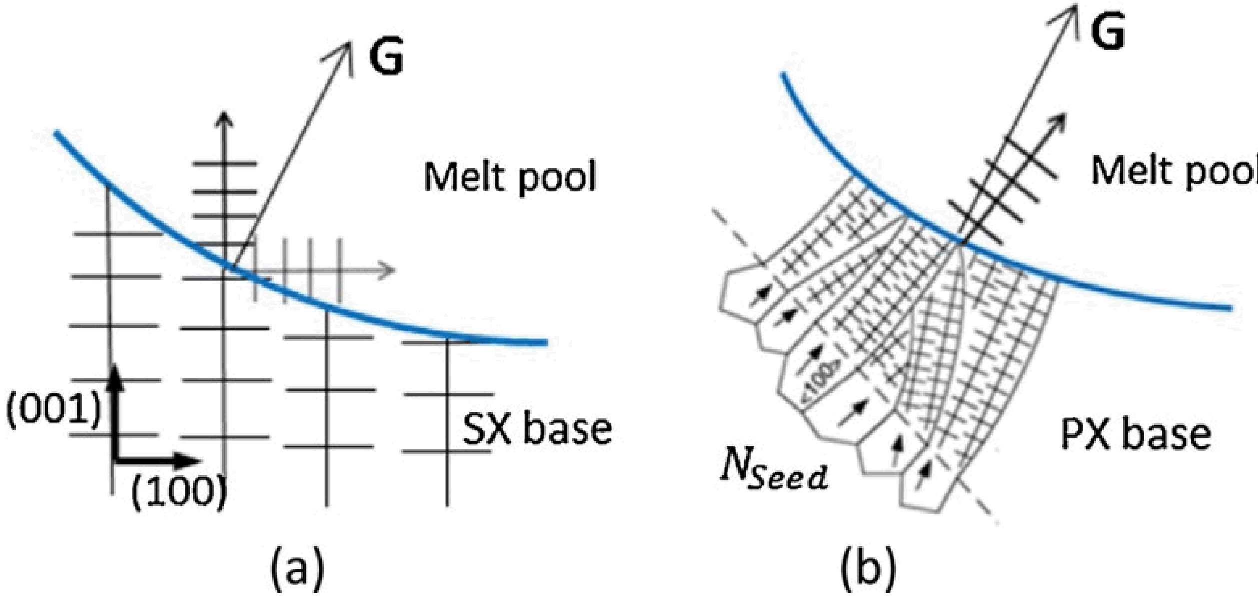

Liu and To, ***Additive Manufacturing* 2017**

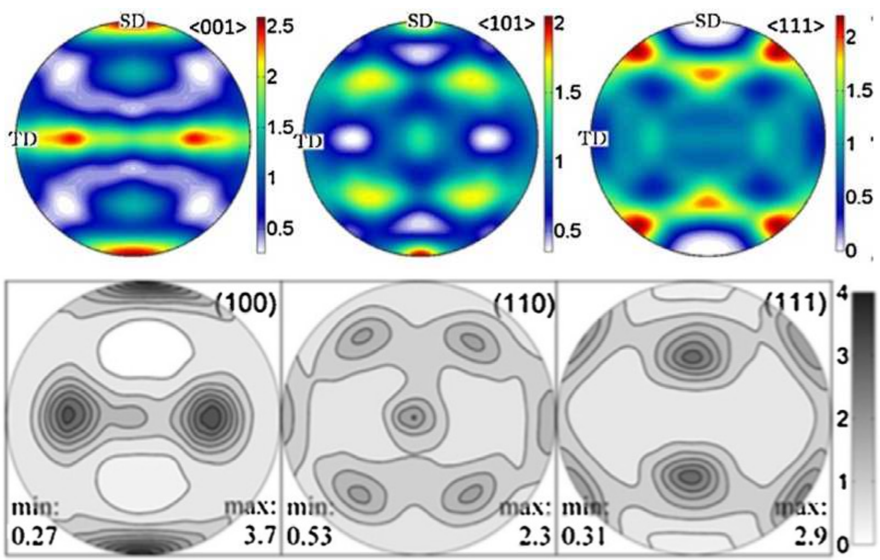

Incorporating anisotropy at the solid/liquid interface

$$M(T) = M_o \exp\left(\frac{-Q}{RT}\right) \qquad Q = Q_o \cos a = Q_o \frac{\boldsymbol{v_{hkl}} \cdot \boldsymbol{G}}{|\boldsymbol{G}|}$$

- Introduce anisotropy through *Q*, activation energy.
- Anisotropy is limited to the "mushy zone" near the solid/liquid interface (no solid/solid anisotropy).
- *Q* is determined by the alignment between <100> crystal directions and temperature gradient.
  - Highly aligned grains are given large values of *Q*, resulting in low mobilities
  - Low-alignment grains are given small values of *Q*, resulting in high mobilities
- Highly aligned, low-mobility grains serve as seeds for the formation of large high-alignment grains.

Preliminary Results – Simulation set up

- Build geometry of a thin wall with 1 pass per layer.
- Intended to simulate materials with cubic-symmetries, but not parameterized in detail to any specific one.
- Used MTEX Matlab toolbox to analyze results.

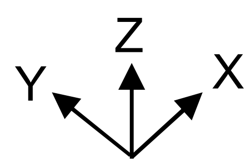

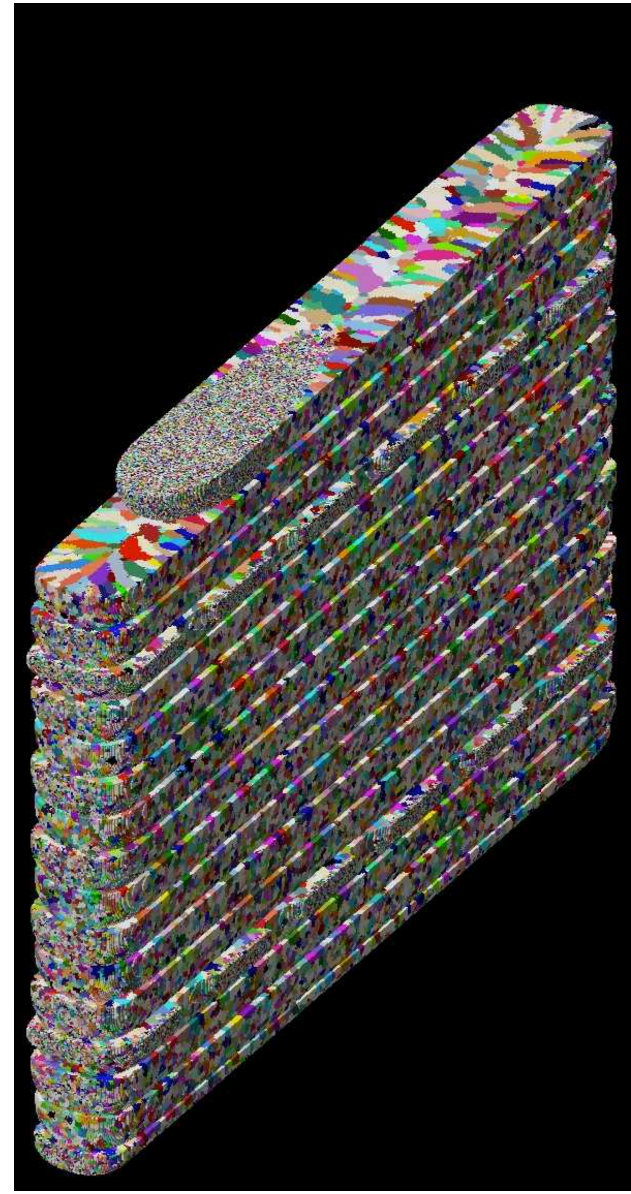

4 V/MCS, 25 V/layer

Constructing EBSD-like coloring

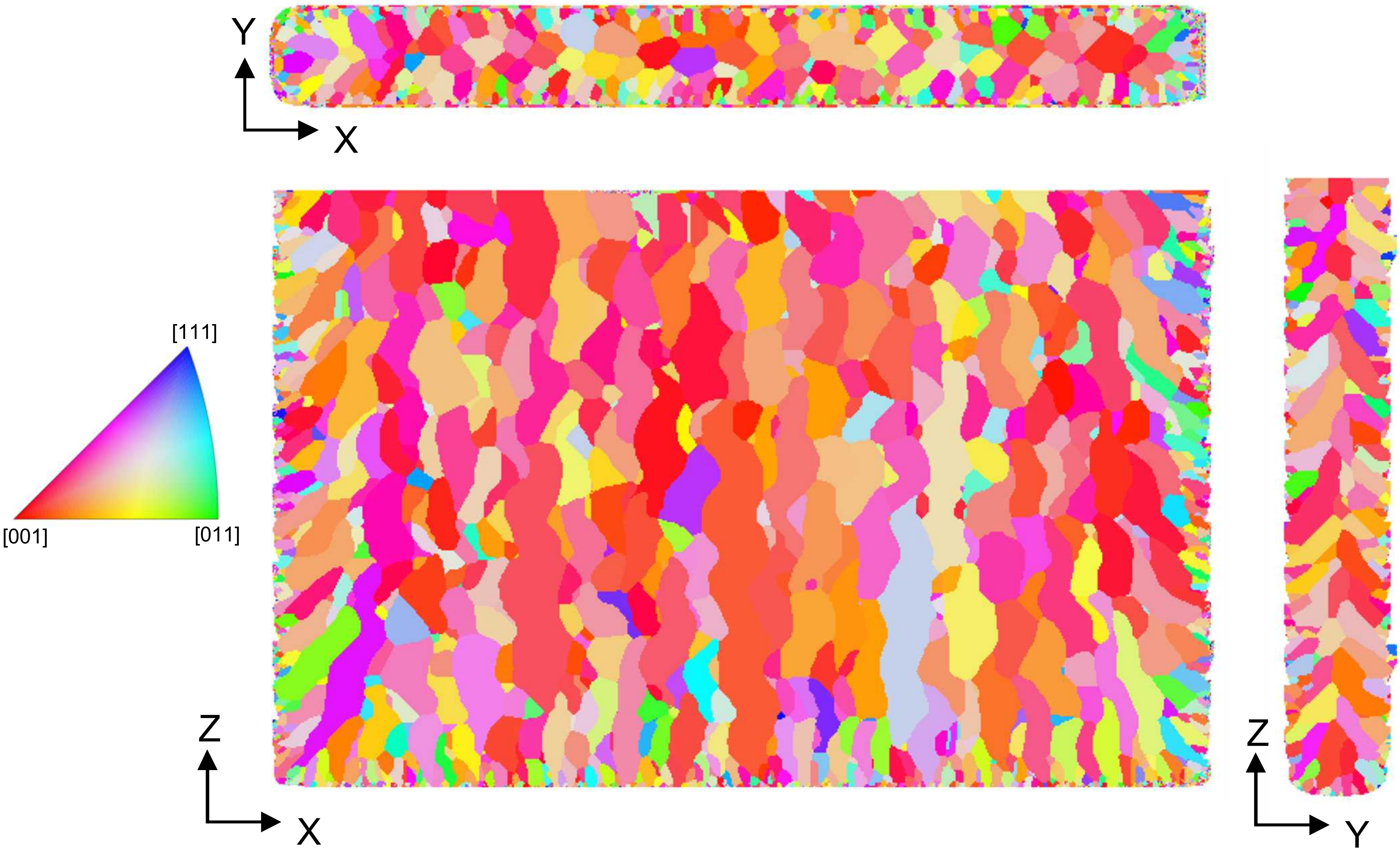

Comparison with experiment

Simulation

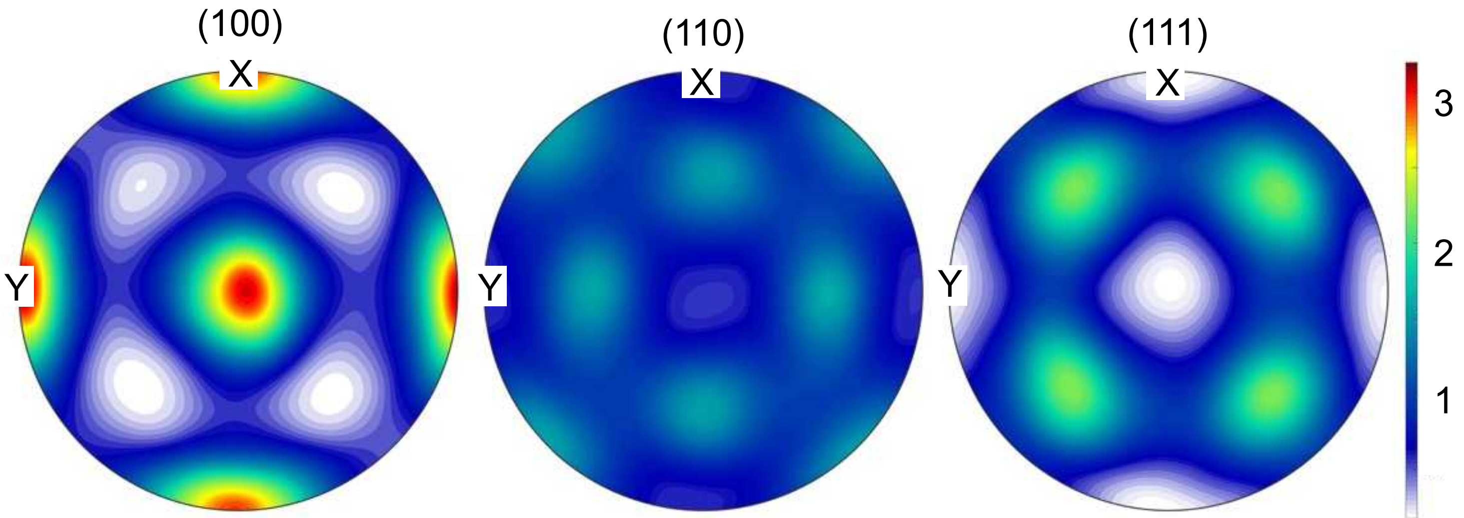

Experiment

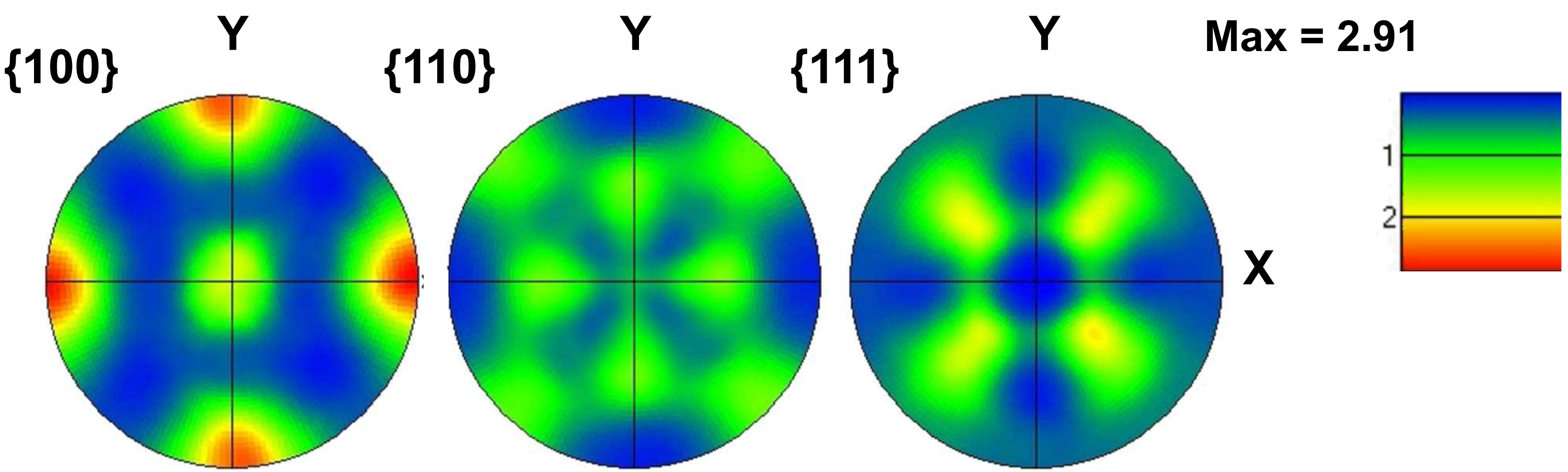

O.D. Underwood, B. Jared, J. Michael, S. Dickens, A. Kilgo, SNL

Outline

- Motivation
- Introduction to Monte Carlo-based microstructure modeling
- Application to solidification problems
- Using synthetic microstructures in further analysis
- Recent & on-going work
  - Utilizing thermal fields from finite element simulations
  - Texture evolution
  - **Finite-difference based thermal diffusion model**
  - Thermofluid model coupling

Coupling thermal diffusion and microstructure evolution

- Solve the heat equation with finite differences

$$\frac{\partial T}{\partial t} - \alpha \nabla^2 T = 0$$

- Heat source modeled as 3D Gaussian.
- Calculate convection radiation or constant *T* boundary conditions in relevant regions.
- Includes latent heat
- Laser path defined externally and implemented with G-code
- Includes “laser off” and recoating times

Incorporating complicated scan strategies

- Use path generation software such as Slic3r or Cura to generate G-code tool paths for heat source.
- Use a Python script to translate G-code into a set of points, which are linearly interpolated between.
- Allows the possibility of simulations using the exact tool paths as experiments.

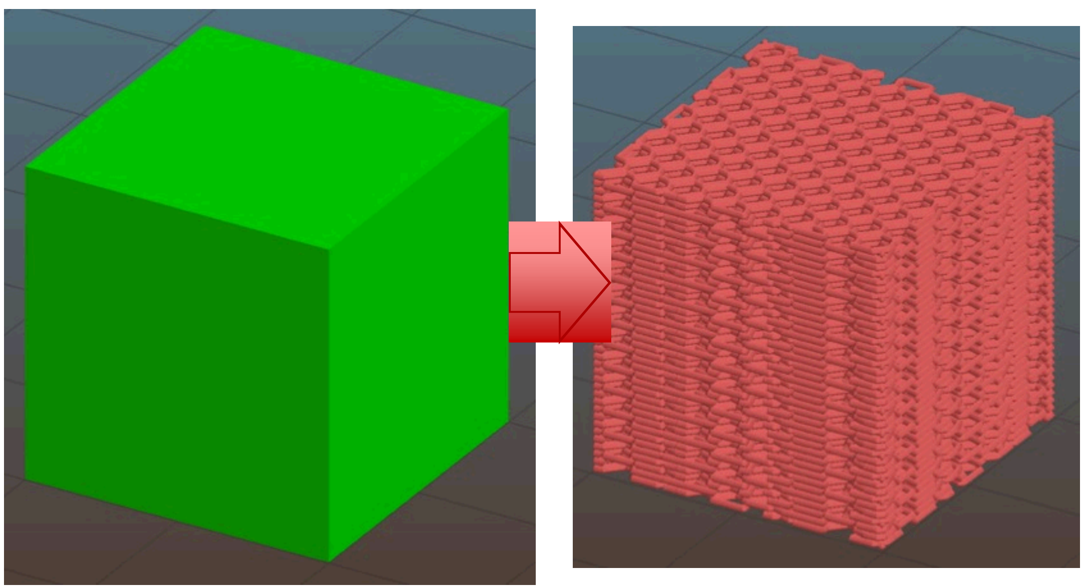

Outline

- Motivation
- Introduction to Monte Carlo-based microstructure modeling
- Application to solidification problems
- Using synthetic microstructures in further analysis
- Recent & on-going work
  - Utilizing thermal fields from finite element simulations
  - Texture evolution
  - Finite-difference based thermal diffusion model
  - **Thermofluid model coupling**

Lattice Boltzmann method: short background

- LBM is derived from cellular automata (CA) algorithms
  - Frisch-Hasslacher-Pomeau discovered that a lattice with hexagonal symmetry can reproduce Navier-Stokes equations
  - Previous square lattices did not have rotational invariance
    - Rotational invariance makes stress tensor isotropic
    - Microdynamics for CA are incorrect but they produce correct macroscopic dynamics
  - Cellular automata's scheme is Boolean
    - Algorithm deals with individual particles
      - A given site is either occupied by a particle or it is empty (yes/no)
      - Leads to large statistical noise
- LBM is an improvement over CA
  - Solves Boltzmann equation
    - Kinetic equation describing thermodynamic systems that are out of equilibrium
  - LBM is not Boolean in nature
  - Uses probability distribution functions

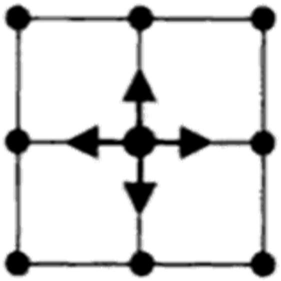

4-link square lattice

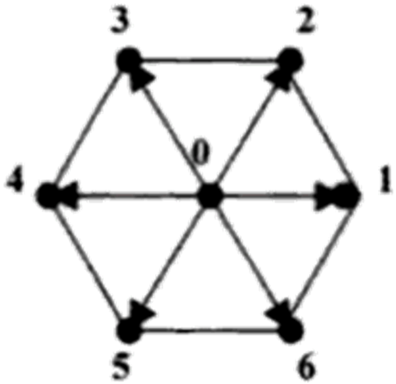

6-link hexagonal lattice

Succi, Sauro. *The lattice Boltzmann equation: for fluid dynamics and beyond*. Oxford university press, 2001.

Thermal Lattice Boltzmann model: 3D results (modeling laser)

Cross-sectional view

phase

solid liquid

Walls and edges are kept at 590ºC

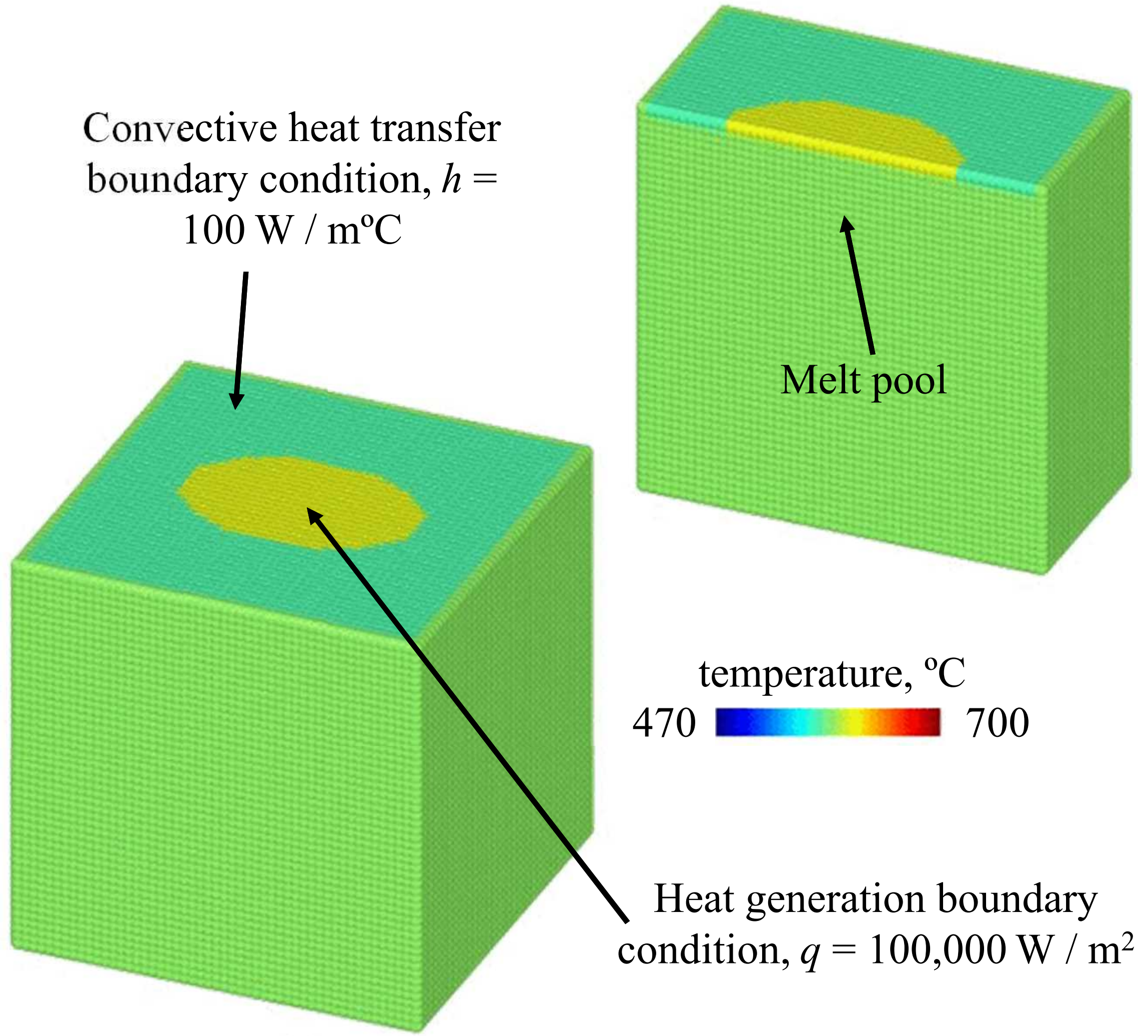

temperature, ºC

470 700

Thermal Lattice Boltzmann model: 3D results (solidification)

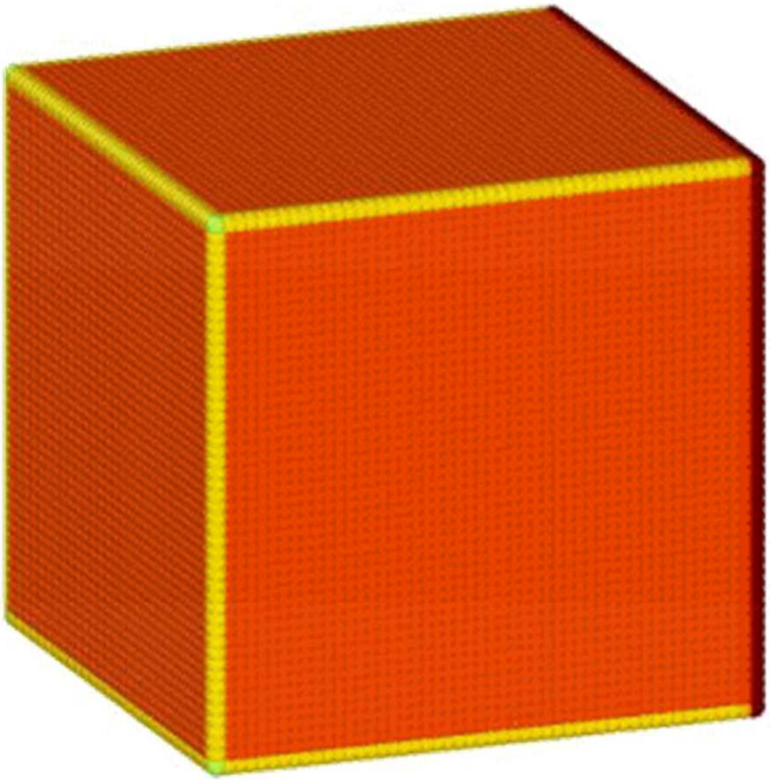

Liquid phase

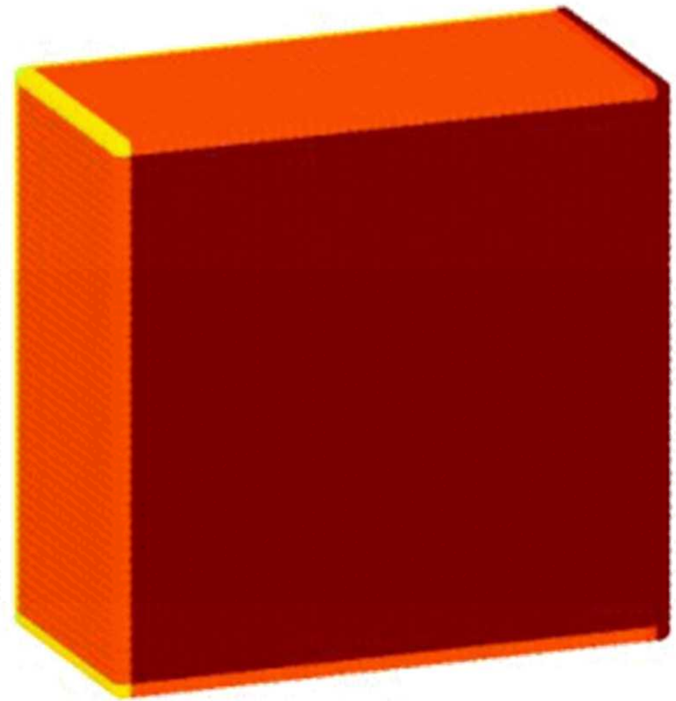

Cross sectional cut through liquid phase

Coupling Hydrodynamic and Thermal models: 2D preliminary results

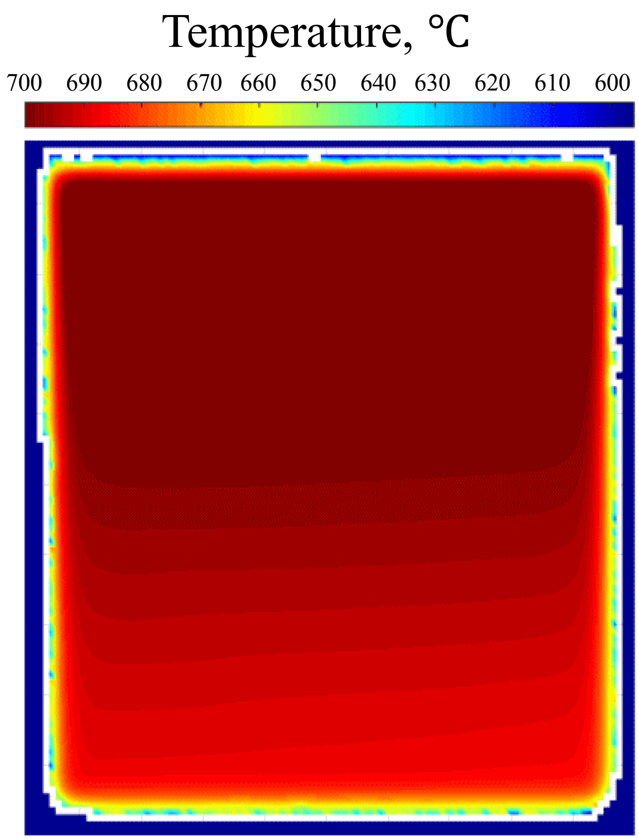

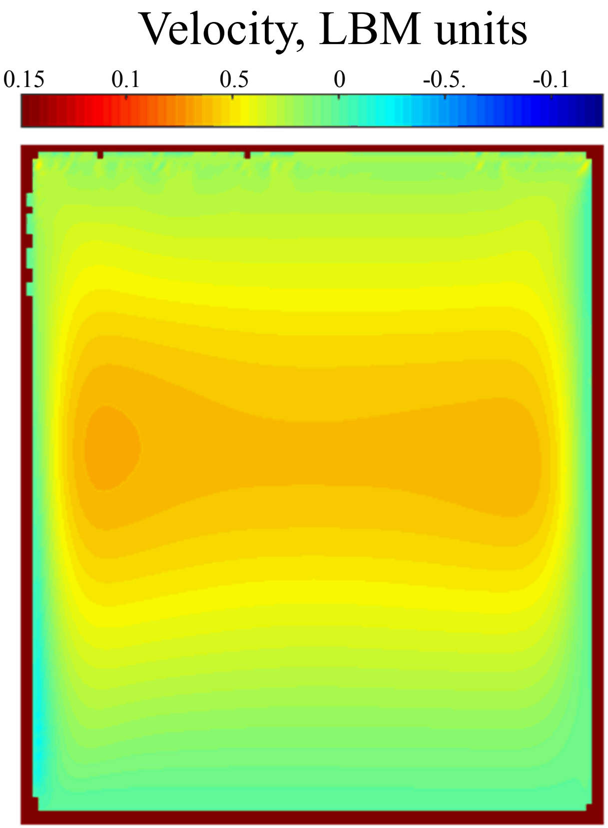

Conclusions

- An open-source 3D microstructure simulation method has been demonstrated for various additive manufacturing and welding applications.
- The simulations can utilize various types of heat sources depending on computational constraints and available data.
- Resulting microstructures can be used in simulations of material performance or as calibration for reduced-order models.
- Additional physics are currently being incorporated into the model.

Backup Slides

Targets for experimental comparison

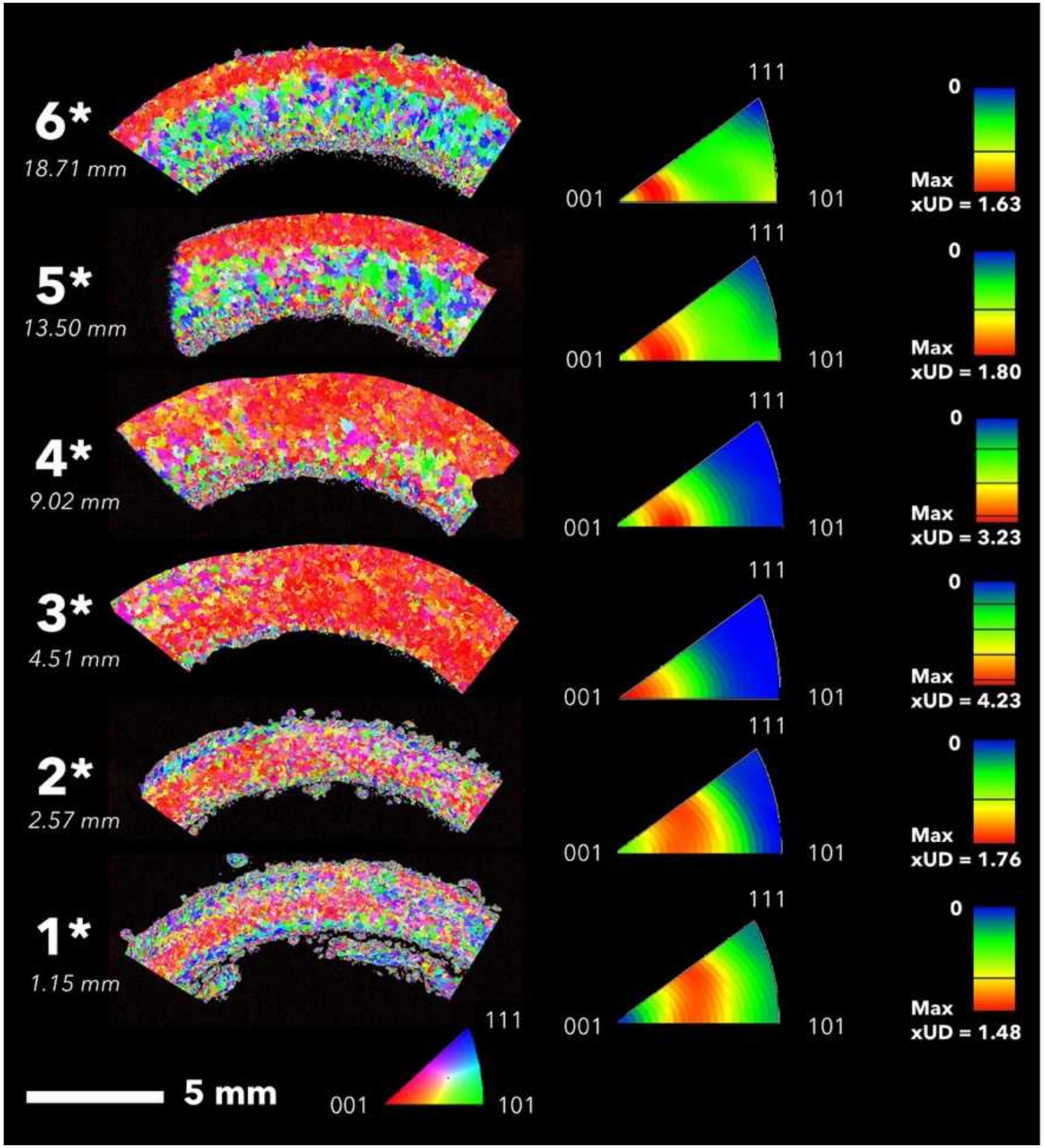

Johnson et al., Under review

Hydrodynamic LBM

- Boltzman equation with BGK collision
  - $\frac{\partial f}{\partial t} + \zeta \cdot \nabla f = \gamma (f^{eq} - f)$
    - ζ is microscopic velocity
    - γ is relaxation parameter
    - f^{eq} is a Boltzmann-Maxwellian distribution function
- Discrete Boltzmann equation with BGK collision
  - $f_i(x, t + \Delta t) = f_i(x,t)(1-\gamma) + \gamma f_i^{eq}(x,t)$
  - $f_i^{eq} = a_i \rho(x,t) \left[1 + \frac{\mathbf{e}_i \cdot \mathbf{u}}{c^2} + \frac{(\mathbf{e}_i \cdot \mathbf{u})^2}{2c^4} - \frac{(\mathbf{u})^2}{2c^2}\right]$, where a_i is a weighing function, ρ is the density, $\mathbf{u}$ is the velocity vector, c is the lattice speed, and e_i is the direction vector
  - $\rho = \sum_{i=1}^{q} f_i$
  - $\mathbf{u} = \frac{1}{\rho} \sum_{i=1}^{q} e_i f_i$
  - pressure = $c^2 \rho$
  - viscosity = $c^2 \rho (1/\gamma - 1/2)$
- Collision → Streaming → Boundary cond.

Discretization of Boltzmann distribution

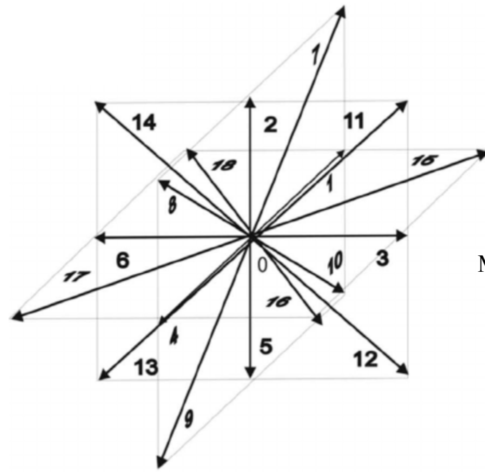

D3Q19 lattice

Luo, K. H., J. Xia, and E. Monaco. "Multiscale modeling of multiphase flow with complex interactions

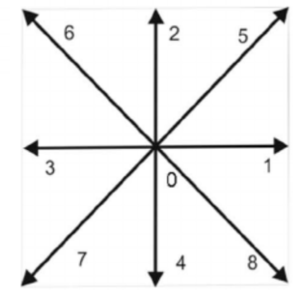

D2Q9 lattice

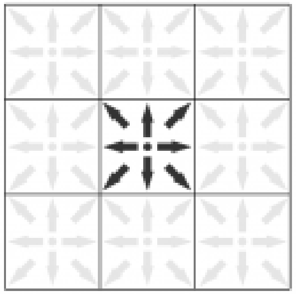

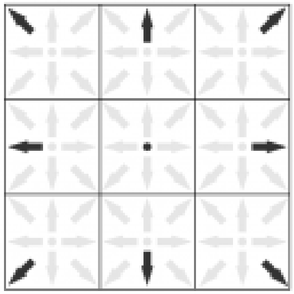

ength distributions (CLDs).

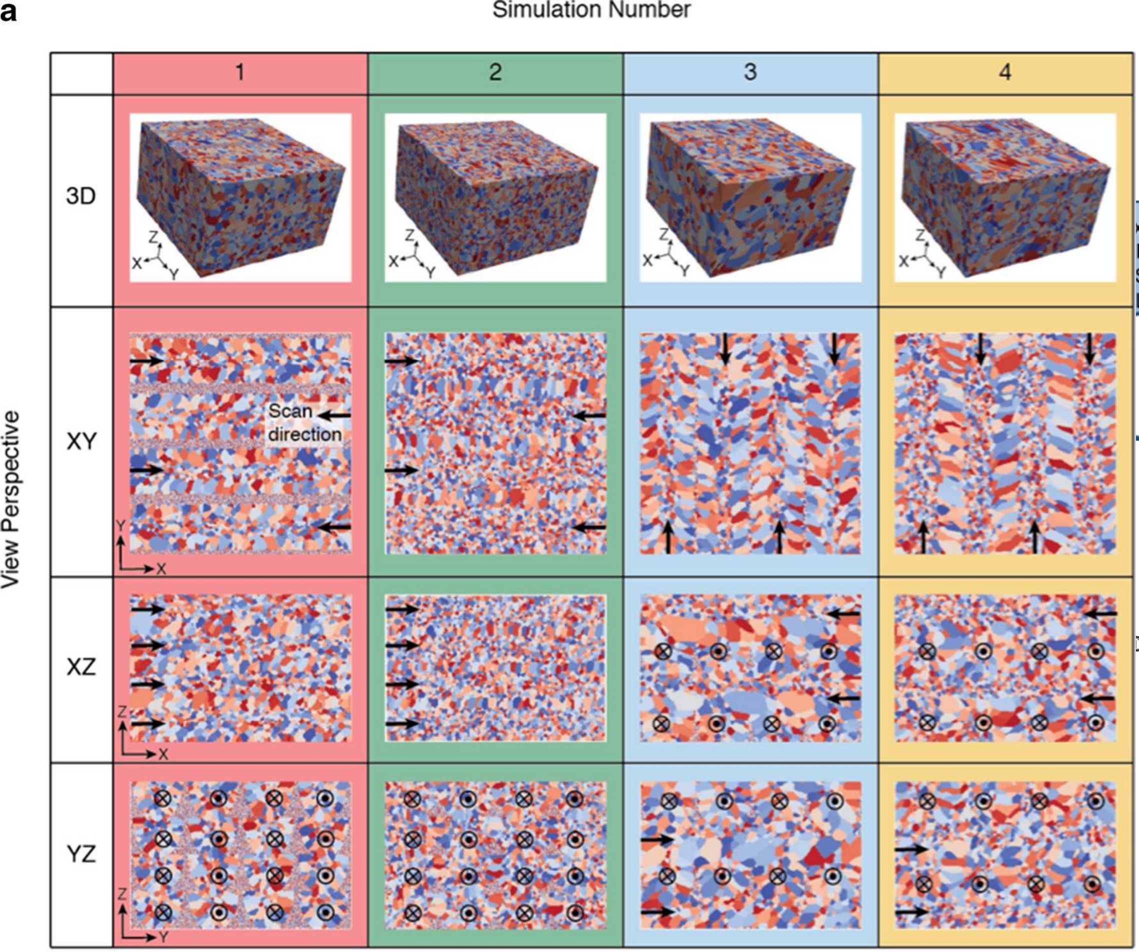

b

Parameter	Simulation Number 1	2	3	4
X/XY	X	X	XY	XY
W	60	80	70	90
V	5	15	5	7.5
D	50	50	62.5	62.5
L	50	60	60	70
HAZ	5	5	20	35
T	5	20	20	35

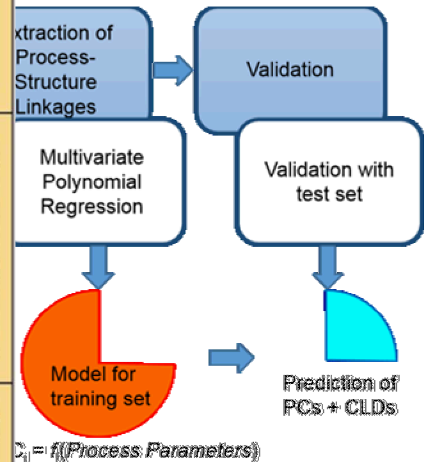

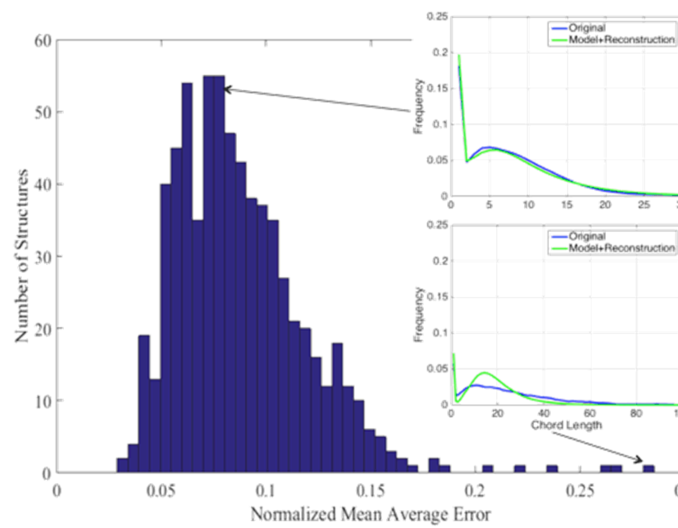

Thermal Lattice Boltzmann model: 2D results

- Top and right walls are kept at 1000ºC and left and bottom walls are kept at 500ºC
- Solidus and liquidus temperatures are set at 596ºC and 652ºC respectively
- c_p = 500 J / kgºC
- k = 30 W / mºC
- L = 271.3 x 10^3 J / kg
- Mushy region represents solid-liquid interface
  - Interface size / properties strongly dependent on liquidus and solidus temperatures

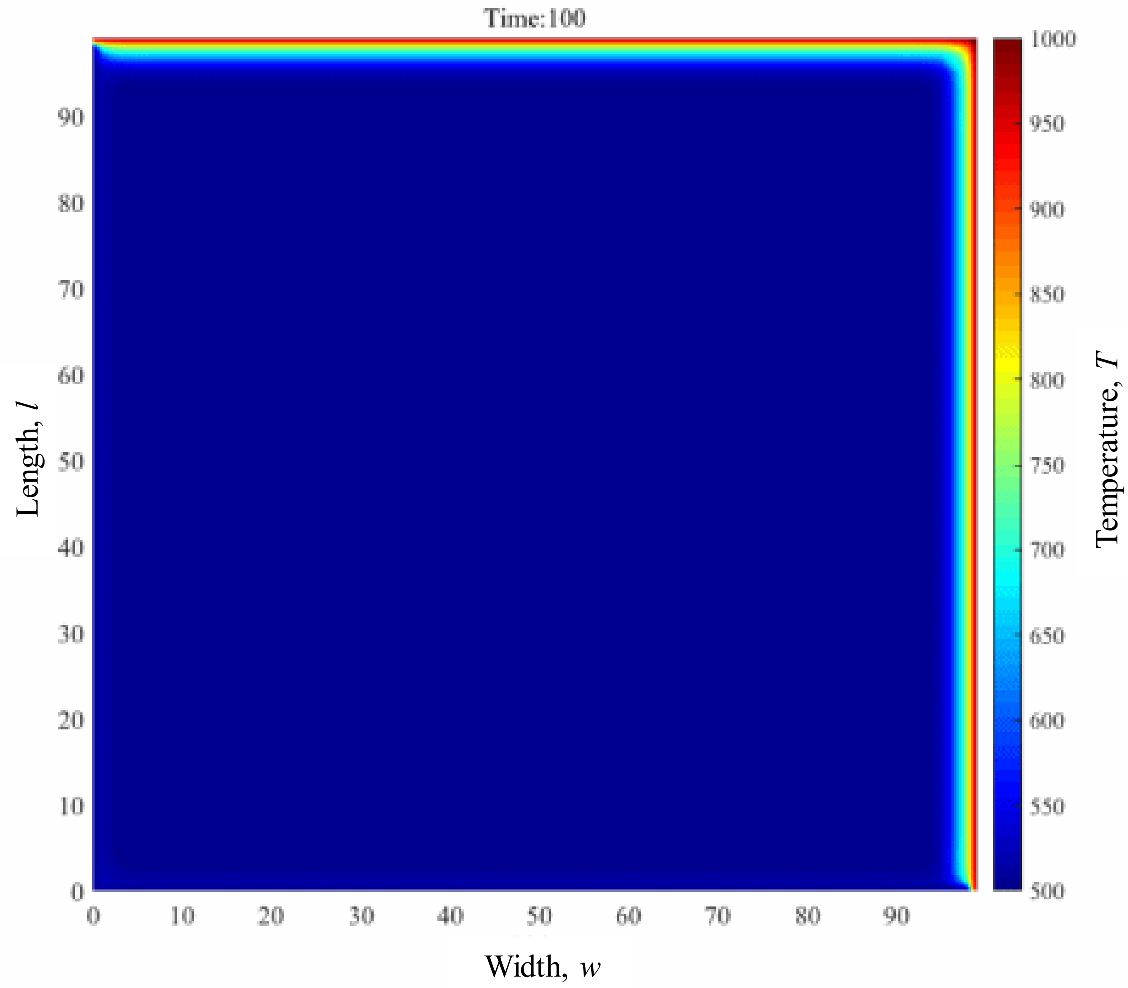

Thermal Lattice Boltzmann model: 3D results (solidification)

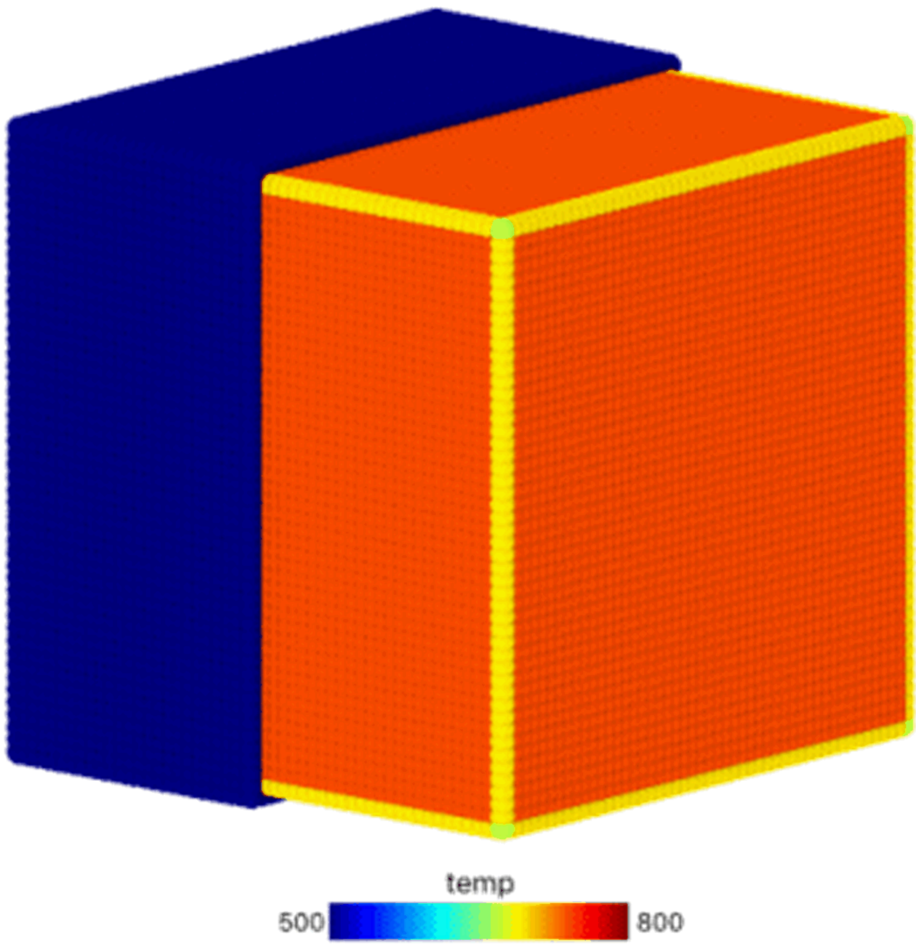

Cross sectional cut through solid phase

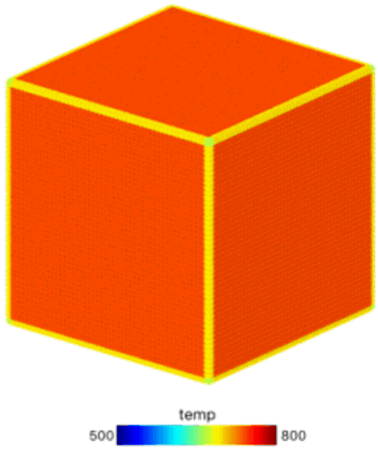

Liquid phase

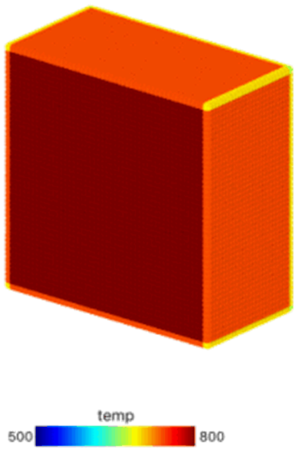

Cross sectional cut through liquid phase

Thermal Lattice Boltzmann model: 3D results (melting)

Initial temperature is 500ºC and walls are kept at 800ºC

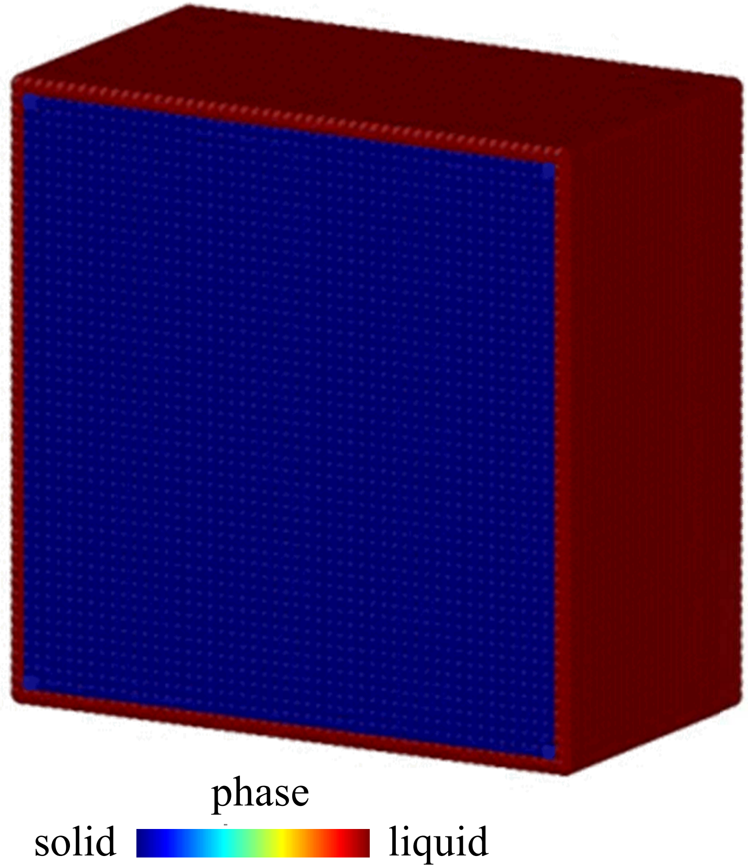

Cross-sectional view of domain

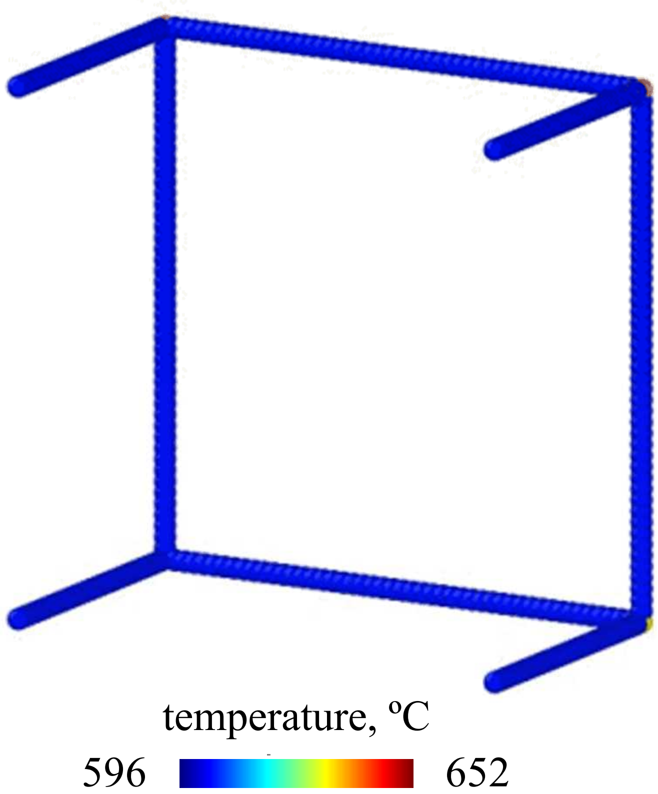

Cross-sectional view of interface

Coupling Hydrodynamic and Thermal models

- Thermo-fluid coupling
  - Thermal equilibrium distribution function
    - $g_i^{eq} = a_i T(x,t)\left[1 + \frac{\boldsymbol{e}_i \cdot \mathbf{u}}{c^2} + \frac{(\boldsymbol{e}_i \cdot \mathbf{u})^2}{2c^4} - \frac{(\mathbf{u})^2}{2c^2}\right]$
  - Natural convection formulation
  - $F_i = a_i\left(1 - \frac{1}{2}\gamma\right)\left(\frac{\boldsymbol{e}_i - \mathbf{u}}{c^2} + \frac{\boldsymbol{e}_i \cdot \mathbf{u}}{c^4}\boldsymbol{e}_i\right) \cdot \rho\left(\mathbf{G}\beta\left(T - T_{ref}\right)\right)$
    - Where β is the volume expansivity and $\boldsymbol{G}$ is the acceleration of gravity
    - Forcing term, $\Delta t F_i$ added to collision of hydrodynamic model
  - Boundary conditions for solid liquid interface
    - Collision operator is modified according to method developed by Noble *et al.*
      - Including modification by Holdych *et al.*
  - $f_i(x, t + \Delta t) = f_i(x,t) - \gamma\Delta t(1 - B)\left(f_i(x,t) - f_i^{eq}(x,t)\right) + (1 - B)\Delta t F_i + B\Omega_i^S$
  - $\Omega_i^S = f_{-i}(x,t) - f_{-i}^{eq}(\rho, \mathrm{u}_S) + f_i^{eq}(\rho, \mathrm{u}_S) - f_i(x,t)$
  - B is weighing function which depends on volume fraction